

¹ The Evolution of Siphonophore Tentilla as Specialized Tools for Prey Capture

³ Alejandro Damian-Serrano^{1,‡}, Steven H.D. Haddock², Casey W. Dunn¹

⁴ ¹ Yale University, Department of Ecology and Evolutionary Biology, 165 Prospect St.,
⁵ New Haven, CT 06520, USA

⁶ ² Monterey Bay Aquarium Research Institute, 7700 Sandholdt Rd., Moss Landing, CA
⁷ 95039, USA

⁸ [‡] Corresponding author: Alejandro Damian-Serrano, email: alejandro.damianserrano@
⁹ yale.edu

¹⁰ Abstract

¹¹ Predators have evolved dedicated body parts to capture and subdue prey. As different
¹² predators specialize on distinct prey taxa, their tools for prey capture diverge into a variety
¹³ of adaptive forms. Studying the evolution of predation is greatly facilitated by a predator
¹⁴ clade with structures used exclusively for prey capture that present significant morphological
¹⁵ variation. Siphonophores, a clade of colonial cnidarians, satisfy these criteria particularly
¹⁶ well, capturing prey with their tentilla (tentacle side branches). Earlier work has shown that
¹⁷ extant siphonophore diets correlate with the different morphologies and sizes of their tentilla
¹⁸ and nematocysts. We hypothesize that evolutionary specialization on different prey types has
¹⁹ driven the phenotypic evolution of these characters. To test this hypothesis, we: (1) measured
²⁰ multiple morphological traits from fixed siphonophore specimens using microscopy and high
²¹ speed video techniques, (2) built a phylogenetic tree of 45 species, and (3) characterized
²² the evolutionary associations between siphonophore nematocyst characters and prey type
²³ data from the literature. Our results show that siphonophore tentillum structure has strong
²⁴ evolutionary associations with prey type and size specialization, and suggest that shifts
²⁵ between prey-type specializations are linked to shifts in tentillum and nematocyst size and

²⁶ shape. In addition, we generated hypotheses about the diets of understudied siphonophore
²⁷ species based on these characters. Thus, the evolutionary history of tentilla shows that
²⁸ siphonophores are an example of ecological niche diversification via morphological innovation
²⁹ and evolution. This study contributes to understanding how morphological evolution has
³⁰ shaped present-day oceanic food-webs.

³¹ **Keywords**

³² Siphonophores, tentilla, nematocysts, predation, specialization, character evolution

³³

³⁴ Most animal predators have characteristic biological tools that they use to capture and
³⁵ subdue prey. Raptors have claws and beaks, snakes have fangs, wasps have stingers, and
³⁶ cnidarians have nematocyst-laden tentacles. The functional morphology of these structures
³⁷ tend to be finely attuned to their ability to successfully capture specific prey (Schmitz
³⁸ 2017). Long-term adaptive evolution in response to the defense mechanisms of the prey (*e.g.*
³⁹ avoidance, escape, protective barriers) leads to modifications that can counter those defenses
⁴⁰ The more specialized the diet of a predator is, the more specialized its tools need to be to
⁴¹ meet the specific challenges posed by the prey. Understanding the relationships between
⁴² predatory specializations and morphological specializations is necessary to contextualize the
⁴³ phenotypic diversity of predators, and to quantify the importance of ecological diversification
⁴⁴ in generating this diversity.

⁴⁵ Siphonophores (Cnidaria : Hydrozoa) are a clade of organisms bearing modular structures
⁴⁶ that are exclusively used for prey capture: the tentilla (Fig. 1). These present a significant
⁴⁷ morphological variation across species (Mapstone 2014) (Fig. 2), which makes it ideal to study
⁴⁸ the relationships between functional traits and prey specialization. A siphonophore is a colony
⁴⁹ bearing many feeding polyps (Fig. 1), each with a single tentacle, which branches into several
⁵⁰ tentilla carrying the functional cnidocytes (specialized neural cells carrying nematocysts,

51 the stinging capsules). Unlike most other cnidarians, siphonophores carry their tentacle
52 nematocysts in extremely complex and organized batteries (Skaer 1988), built into their
53 tentilla. While nematocyst batteries and clusters in other cnidarians are simple static scaffolds
54 for cnidocytes, siphonophore tentilla have their own reaction mechanism, triggered upon
55 encounter with prey. When it fires, a tentillum undergoes an extremely fast conformational
56 change that wraps it around the prey, maximizing the surface area of contact for nematocysts
57 to fire on the prey (Mackie et al. 1987). In addition, some species have elaborate fluorescent
58 and bioluminescent lures on their tentilla to attract prey with aggressive mimicry (Purcell
59 1980; Haddock et al. 2005; Haddock and Dunn 2015).

60 Many siphonophore species inhabit the deep pelagic ocean, which spans from ~200m to
61 the oceanic seafloor. This habitat has fairly homogeneous physical conditions and stable
62 abundances of zooplanktonic animals (Robison 2004). With a relatively predictable prey
63 availability, ecological theory would predict evolution to drive coexisting siphonophore
64 lineages towards specialization, increasing their feeding efficiencies and reducing interspecific
65 competition (Hardin 1960; Hutchinson 1961). If this prediction holds true, we expect the prey
66 capture apparatus morphologies of siphonophores to diversify with the evolution of increased
67 specialization on a variety of prey types in different siphonophore lineages.

68 Coexisting siphonophores feeding on the same planktonic community may have substantial
69 niche overlap and compete for prey resources. Traditional ecological coexistence theory
70 (Simpson 1944) predicts that competition between species would select for increasing ecological
71 specialization. This specialization is often thought to be an evolutionary ‘dead end’, meaning
72 that specialized lineages are unlikely to evolve into generalists or to shift the resource for
73 which they are specialized (Futuyma and Moreno 1988). However, recent studies have found
74 that interspecific competition can favor the evolution of resource generalism (Stireman-III
75 2005; Johnson et al. 2009) and resource switching (Hoberg and Brooks 2008). Here we
76 examine three alternative hypotheses on siphonophore trophic specialization: (1) predatory
77 specialists evolved from generalist ancestors; (2) predatory specialists evolved from ancestral

78 predatory specialists which specialized on a different resource, switching their primary prey
79 type; and (3) predatory generalists evolved from specialist ancestors.

80 The study of siphonophore tentilla and diets has been limited in the past due to the
81 inaccessibility of their oceanic habitat and the difficulties associated with the collection of
82 fragile siphonophores. Thus, the morphological diversity of tentilla has only been characterized
83 for a few taxa, and their evolutionary history remains largely unexplored. Contemporary
84 underwater sampling technology provides an unprecedented opportunity to explore the trophic
85 ecology (Choy et al. 2017) and functional morphology (Costello et al. 2015) of siphonophores.
86 In addition, well-supported phylogenies based on molecular data are now available for these
87 organisms (Munro et al. 2018). These advances allow for the examination of relationships
88 between modern siphonophore form, function, and ecology, as well as reconstructing their
89 evolutionary history.

90 The few pioneering studies that have addressed the relationships between tentilla and
91 diet suggest that siphonophores are a robust system for the study of predatory specialization
92 via morphological diversification. (Purcell 1984) and (Purcell and Mills 1988) showed clear
93 relationships between diet, tentillum, and nematocyst characters in co-occurring epipelagic
94 siphonophores. These correlations, while studied for a small subset of extant epipelagic
95 siphonophore species, might be generalizable to all siphonophores. We hypothesize that
96 these relationships reflect correlated evolution between prey selection and tentillum (and
97 nematocyst) traits. Furthermore, we hypothesize that with an extensive characterization of
98 tentilla morphology, we can generate hypotheses about the diets of understudied siphonophore
99 species. In addition, our study design allows us to address other interesting questions about
100 the morphology and evolution of these unique structures. In particular, we aim to address
101 the evolutionary origins of giant tentilla, the phenotypic integration of tentilla, the evolution
102 of the extreme shapes of siphonophore haploneme nematocysts (Thomason 1988), and the
103 mechanical implications of tentillum morphologies on cnidoband discharge.

104 In this study, we characterize the morphological diversity of tentilla and their nematocysts

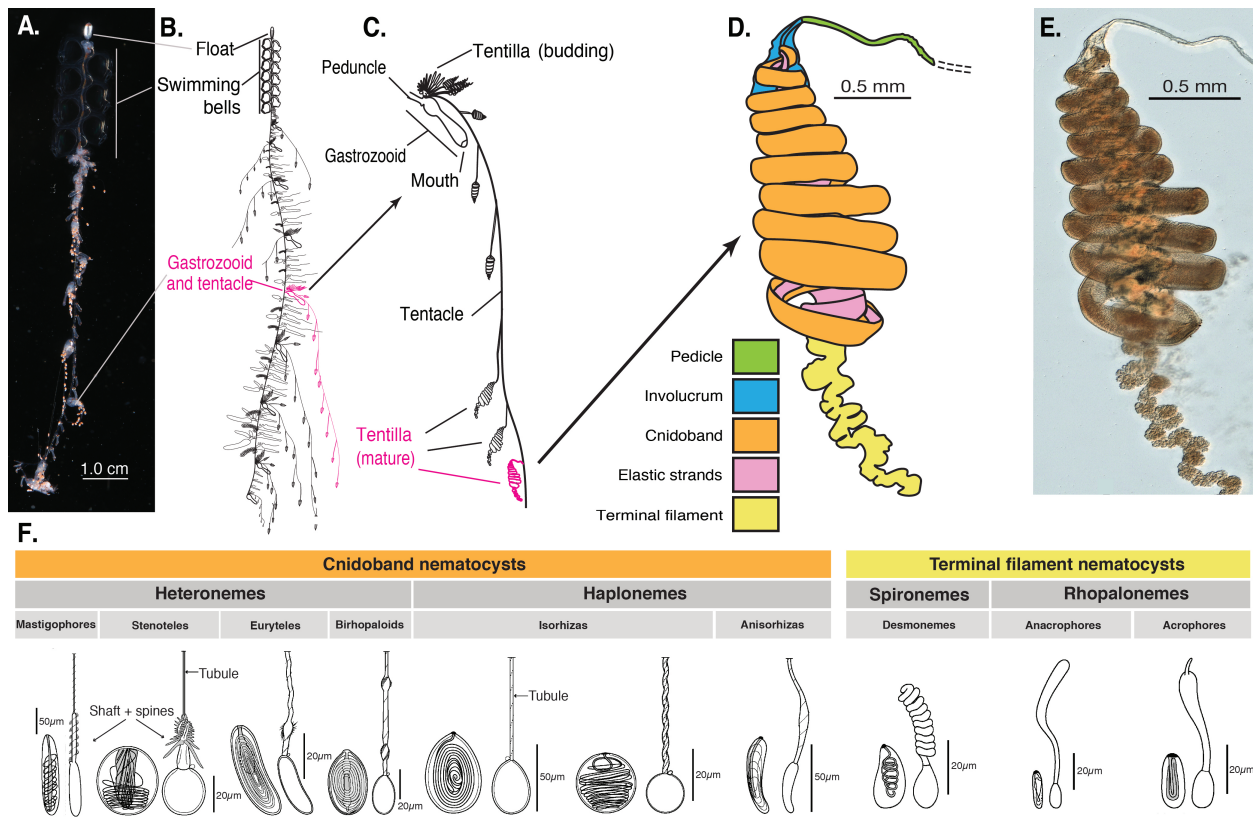


Figure 1: Siphonophore anatomy. A - *Nanomia* sp. siphonophore colony (photo by Catriona Munro). B,C - Illustration of a *Nanomia* colony, gastrozooid, and tentacle (by Freya Goetz). D - *Nanomia* sp. Tentillum illustration and main parts. E - Transmission micrograph of the tentillum illustrated in D. F - Nematocyst types (illustration reproduced with permission from Mapstone 2014), hypothesized homologies, and locations in the tentillum. Undischarged to the left, discharged to the right.

105 across a broad variety of shallow and deep sea siphonophore species using modern imaging
 106 technologies, we expand the phylogenetic tree of siphonophores by combining a broad taxon
 107 sampling of ribosomal gene sequences with a transcriptome-based backbone tree, and we
 108 explore the evolutionary histories and correlations among diet, tentillum, and nematocyst
 109 characters.

110 Methods

111 *Tentillum morphology* – The morphological work was carried out on siphonophore specimens
 112 fixed in 4% formalin from the Yale Peabody Museum Invertebrate Zoology (YPM-IZ) collection

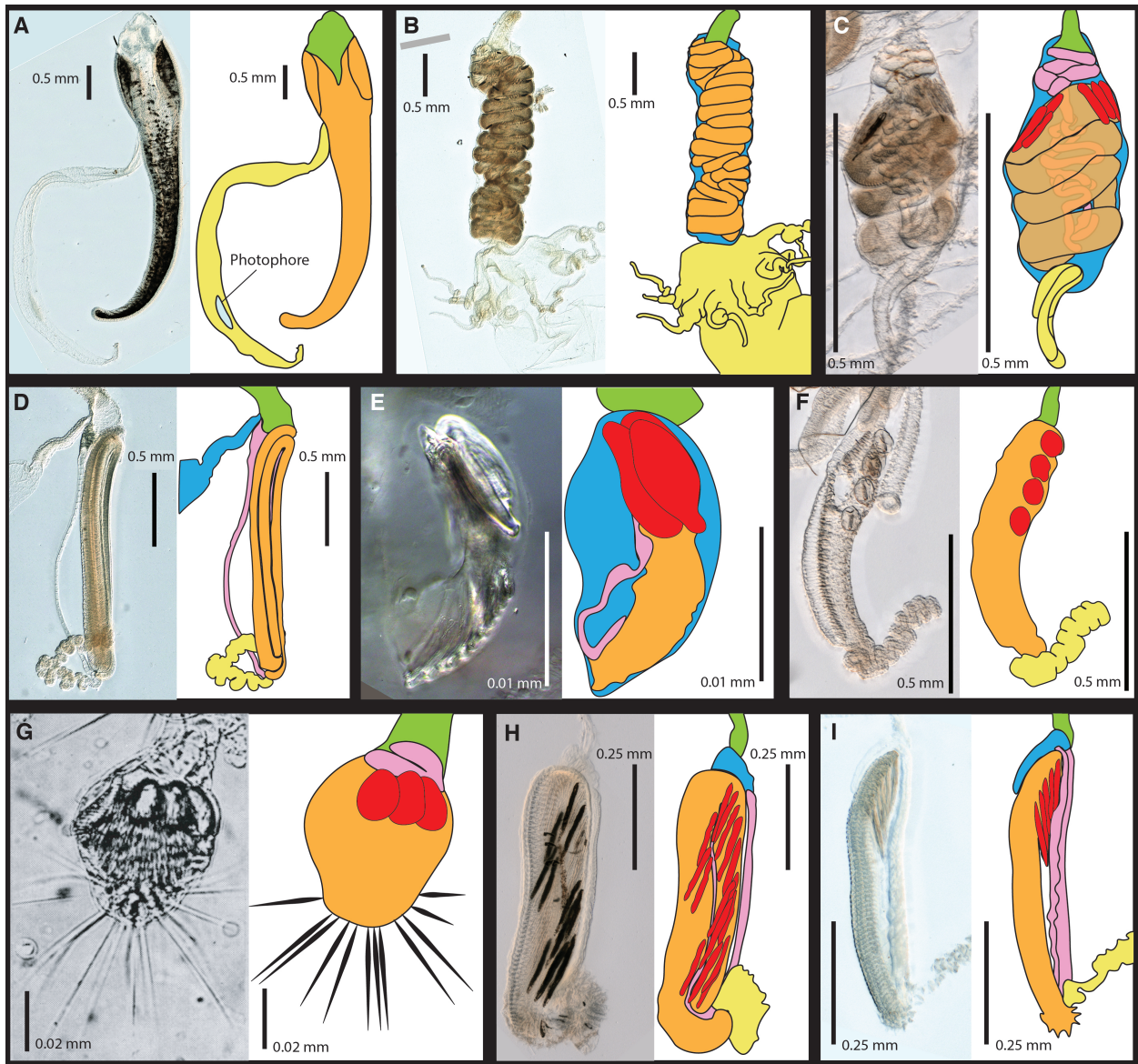


Figure 2: Tentillum diversity plate. The illustrations delineate the pedicle (green), involucrum (blue), cnidoband (orange), elastic strands (pink), terminal structures (yellow). Heteroneme nematocysts (stenoteles in C,E,F,G and mastigophores in H,I) are depicted in red for some species. A - *Erenna laciniata*, 10x. B - *Lychnagalma utricularia*, 10x. C - *Agalma elegans*, 10x. D - *Resomia ornicephala*, 10x. E - *Frillagalma vityazi*, 20x. F - *Bargmannia amoena*, 10x. G - *Cordagalma* sp., reproduced from Carré 1968. H - *Lilyopsis fluoracantha*, 20x. I - *Abylopsis tetragona*, 20x.

113 (accession numbers in Appendix 1). These specimens were collected intact across many years
114 of fieldwork expeditions, using blue-water diving (Haddock and Heine 2005), remotely
115 operated vehicles (ROVs), and human-operated submersibles. Tentacles were dissected
116 from non-larval gastrozooids, sequentially dehydrated into 100% ethanol, cleared in methyl
117 salicylate, and mounted into slides with Canada Balsam or Permount mounting media. The
118 slides were imaged as tiled z-stacks using differential interference contrast (DIC) on an
119 automated stage at YPM-IZ (with the assistance of Daniel Drew and Eric Lazo-Wasem) and
120 with laser point confocal microscopy using a 488 nm Argon laser that excited autofluorescence
121 in the tissues. Thirty characters (defined in Appendix 2) were measured using Fiji (Collins
122 2007; Schindelin et al. 2012). We did not measure the lengths of contractile structures
123 (terminal filaments, pedicles, gastrozooids, and tentacles), since they are too variable to
124 quantify. We measured at least one specimen for 96 different species (Appendix 3, Fig.
125 3). Of these, we selected 38 focal species across clades based on specimen availability and
126 phylogenetic representation. Three to five tentacle specimens from each one of these selected
127 species were measured to capture intraspecific variation.

128 In order to observe the discharge behavior of different tentilla, we recorded high speed
129 footage (1000-3000 fps) of tentillum and nematocyst discharge by live siphonophore specimens
130 (26 species) using a Phantom Miro 320S camera mounted on a stereoscopic microscope. We
131 mechanically elicited tentillum and nematocyst discharge using a fine metallic pin. We used
132 the Phantom PCC software to analyze the footage. For the 10 species recorded, we measured
133 total cnidoband discharge time (ms), heteroneme filament length (μm), and discharge speeds
134 (mm/s) for cnidoband, heteronemes, haplonemes, and heteroneme shafts when possible (data
135 in Appendix 4).

136 *Siphonophore phylogeny* – The phylogenetic analysis included 55 siphonophore species
137 and 6 outgroup cnidian species (*Clytia hemisphaerica*, *Hydra circumcincta*, *Ectopleura*
138 *dumortieri*, *Porpita porpita*, *Velella velella*, *Staurocladia wellingtoni*). The gene sequences
139 we used in this study are available online (accession numbers in Appendix 5). Some of

the sequences we used were accessioned in (Dunn et al. 2005), and others we extracted from the transcriptomes in (Munro et al. 2018). Two new 16S sequences for *Frillagalma vityazi* (MK958598) and *Thermopalia* sp. (MK958599) sequenced by Lynne Christianson were included and accessioned to NCBI. We aligned these sequences using MAFFT (Katoh et al. 2002) (alignments available in Dryad). We inferred a Maximum Likelihood (ML) phylogeny (Appendix 6) from 16S and 18S ribosomal rRNA genes using IQTree (Nguyen et al. 2014) with 1000 bootstrap replicates (iqtree -s alignment.fa -nt AUTO -bb 1000). We used ModelFinder (Kalyaanamoorthy et al. 2017) implemented in IQTree v1.5.5. to assess relative model fit. ModelFinder selected GTR+R4 for having the lowest Bayesian Information Criterion score. Additionally, we inferred a Bayesian tree with each gene as an independent partition in RevBayes (Höhna et al. 2016) (Appendix 7 and 9), which was topologically congruent with the unconstrained ML tree. The *alpha* priors were selected to minimize prior load in site variation.

Given the broader sequence sampling of the transcriptome phylogeny, we ran constrained inferences (using both ML and Bayesian timetree approaches, which produced fully congruent topologies (Appendix 6 and 7)) after fixing the 5 nodes that were incongruent with the topology of the consensus tree in (Munro et al. 2018). This topology was then used to inform a Bayesian relaxed molecular clock time-tree in RevBayes, using a birth-death process (sampling probability calculated from the known number of described siphonophore species) to generate ultrametric branch lengths (Appendix 8). Scripts available in Appendix 9.

Feeding ecology – We extracted categorical diet data for different siphonophore species from published sources, including seminal papers (Biggs 1977; Purcell 1981, 1984; Andersen 1981; Mackie et al. 1987; Pugh and Youngbluth 1988; Bardi and Marques 2007), and ROV observation data (Hissmann 2005; Choy et al. 2017) with the assistance of Elizabeth Hetherington and Anela Choy (Appendix 10). We removed the gelatinous prey observations for *Praya dubia* eating a ctenophore and a hydromedusa, and for *Nanomia* sp. eating *Aegina*, since we believe these are rare events that have a much larger probability of being detected by ROV

methods than their usual prey, and it is not clear whether the medusae were attempting to prey upon the siphonophores. Personal observations on feeding (from SHDH, CAC, and Philip Pugh) were also included for *Resomia ornicephala*, *Lychnagalma utricularia*, *Bargmannia amoena*, *Erenna richardi*, *Erenna laciniata*, *Erenna sirena*, and *Apolemia rubriversa*. In order to detect coarse-level patterns in the feeding habits, the data were merged into feeding guilds. The feeding guilds described here are: small-crustacean specialist (feeding mainly on copepods and ostracods), large crustacean specialist (feeding on large decapods, mysids, or krill), fish specialist (feeding mainly on actinopterygian larvae, juveniles, or adults), gelatinous specialist (feeding mainly on other siphonophores, medusae, ctenophores, salps, and/or doliolids), and generalist (feeding on a combination of the aforementioned taxa, without favoring any one prey group). These were selected to minimize the number of categories while keeping the most different types of prey separate. We extracted copepod prey length data from (Purcell 1984). To calculate specific prey selectivities, we extracted quantitative diet and zooplankton composition data from (Purcell 1981), matched each diet assessment to each prey field quantification by site, calculated Ivlev's electivity indices (Jacobs 1974), and averaged those by species (Appendix 11).

Statistical analyses – For subsequent comparative analyses, we removed species present in the tree but not represented in the morphology data, and *vice versa*. Although we measured specimens labeled as *Nanomia bijuga* and *Nanomia cara*, we are not confident in some of the species-level identifications, and some specimens were missing diagnostic zooids. Thus, we decided to collapse these into a single taxonomic concept (*Nanomia* sp.). All *Nanomia* sp. observations were matched to the phylogenetic position of *Nanomia bijuga* in the tree. We carried out all phylogenetic comparative statistical analyses in the programming environment R (Team 2017), using the bayesian ultrametric species tree (Fig. 4), and incorporating intraspecific variation estimated from the specimen data as standard error (Appendix 3). R scripts available in Dryad. For each character (or character pair) analyzed, we removed species with missing data and reported the number of taxa included. We tested each character

¹⁹⁴ for normality using the Shapiro-Wilk test (Shapiro and Wilk 1965), and log-transformed
¹⁹⁵ those that were non-normal.

¹⁹⁶ We fitted different models generating the observed data distribution given the phylogeny
¹⁹⁷ for each continuous character using the function `fitContinuous` in the R package *geiger*
¹⁹⁸ (Harmon et al. 2007). The models compared were the white noise (WN; non-phylogenetic
¹⁹⁹ model that assumes all values come from a single normal distribution with no covariance
²⁰⁰ structure among species), the Brownian Motion (BM) model of neutral divergent evolution
²⁰¹ (Martins 1996), the Early Burst (EB) model of decreasing rate of evolutionary change (Harmon
²⁰² et al. 2010), and the Ornstein-Uhlenbeck (OU) model of stabilizing selection around a fitted
²⁰³ optimum state (Uhlenbeck and Ornstein 1930; Butler and King 2004). We then ranked the
²⁰⁴ models in order of increasing parametric complexity (WN,BM,EB,OU), and compared the
²⁰⁵ corrected Akaike Information Criterion (AICc) support scores (Sugiura 1978) to the lowest
²⁰⁶ (best) score, using a cutoff of 2 units to determine significantly better support. When the
²⁰⁷ best fitting model was not significantly better than a less complex alternative, we selected
²⁰⁸ the least complex model (Appendix 12). We calculated model adequacy scores using the
²⁰⁹ R package *arbutus* (Pennell et al. 2015) (Appendix 13). We calculated phylogenetic signal
²¹⁰ in each of the measured characters using Blomberg's K (Blomberg et al. 2003) (Appendix
²¹¹ 12), and for the morphological dataset as a whole using the R package *geomorph* (Adams et
²¹² al. 2016). We reconstructed ancestral states using Maximum Likelihood (`anc.ML` (Revell
²¹³ 2012)), and stochastic character mapping (`make.simmap`) for categorical characters. R scripts
²¹⁴ available in Dryad.

²¹⁵ In order to study the evolution of predatory specialization, we reconstructed components
²¹⁶ of the diet and prey selectivity on the phylogeny using ML (R `phytools::anc.ML`). To identify
²¹⁷ evolutionary associations of diet with tentillum and nematocyst characters, we compared the
²¹⁸ performance of a neutral evolution model to that of a diet-driven directional selection model.
²¹⁹ First, we collapsed the diet data into the five feeding guilds mentioned above (fish specialist,
²²⁰ small crustacean specialist, large crustacean specialist, gelatinous specialist, generalist), based

on which prey types they were observed consuming most frequently. We reconstructed the feeding guild ancestral states using the ML function `ace` (package `ape` (Paradis et al. 2019)), removing tips with no feeding data. The ML reconstruction was congruent with the consensus stochastic character mapping (Appendix 18). Then, using the package `OUwie` (Beaulieu and O'Meara 2012), we fitted an OU model with multiple optima and rates of evolution matched to the reconstructed ancestral diet regimes, a single optimum OU model, and a BM null model, inspired by the analyses in (Cressler et al. 2015). Finally, we compared their AICc support values to select the best fitting model (Appendix 14).

To model the evolutionary associations between individual tentillum and nematocyst characters and the ability to capture particular prey types in the diet, we ran a series of phylogenetic generalized linear models (R `phyloglm`) (Appendix 17). In addition, we ran a series of comparative analyses to address hypotheses of diet-tentillum relationships posed in the literature. To test for correlated evolution among binary characters, we used Pagel's test (Pagel 1994). To characterize and evaluate the relationship between continuous characters, we used phylogenetic generalized least squares regressions (PGLS) (Grafen 1989). To compare the evolution of continuous characters with categorical aspects of the diet, we carried out a phylogenetic logistic regression (R `nlme::gls`).

To generate hypotheses about the diets of understudied siphonophores for which no feeding observations have yet been reported (but for which we have tentacle morphology data), we carried out linear discriminant analysis of principal components (DAPC) using the `dapc` function (R `adegenet::dapc`) (Jombart et al. 2010). This function allowed us to incorporate more predictors than individuals. We generated discriminant functions for feeding guild, soft/hard bodied prey, presence of copepods, fish, and shrimp (large crustaceans) in the diet (Appendix 15). Some taxa have inapplicable states for certain absent characters (such as the length of a nematocyst subtype that is not present in a species), which are problematic for DAPC analyses. We tackled this by transforming the absent states to zeroes. This approach allows us to incorporate all the data, but creates an attraction bias between

248 small character states (*e.g.* small tentilla) and absent states (*e.g.* no tentilla). Absent
249 characters are likely to be very biologically relevant to prey capture and we believe they
250 should be accounted for. We limited the number of linear discriminant functions retained
251 to the number of groupings in each case. We selected the number of principal components
252 retained using the a-score optimization function (R adegenet::optim.a.score) (Jombart et
253 al. 2010) with 100 iterations, which yielded more stable results than the cross validation
254 function (R adegenet::xval). This optimization aims to find the compromise value with highest
255 discrimination power with the least overfitting. From these DAPCs we obtained the highest
256 contributing morphological characters to the discriminaton (characters in the top quartile of
257 the weighted sum of the linear discriminant loadings controlling for the eigenvalue of each
258 discriminant). For each DAPC we generated hypotheses about the diets of siphonophores
259 outside the training set (R adegenet::predict.dapc), incorporating prediction uncertainty as
260 posterior probabilities (Appendix 15). In order to identify the sign of the relationship between
261 the predictor characters prey type presence in the diet, we then generated generalized logistic
262 regression models (as a type of generalized linear model, or GLM using R stats::glm) with the
263 top contributing characters (from the corresponding DAPC) as predictors. We also carried
264 out these GLMs on the Ivlev's selectivity indices for each prey type calculated from (Purcell
265 1981) (in Appendix 11).

266 In order to explore the correlational structure among continuous characters and among
267 their evolutionary histories, we used principal component analysis (PCA) and phylogenetic
268 PCA (Revell 2012). Since the character data contains many gaps due to missing characters
269 and inapplicable states, we carried out these analyses on a subset of species and characters
270 that allowed for the most complete dataset. This was done by removing the terminal filament
271 characters (which are only shared by a small subset of species), and then removing species
272 which had inapplicable states for the remaining characters. In addition, we obtained the
273 correlations between the phylogenetic independent contrasts (Felsenstein 1985) using the
274 package rphylip (Revell and Chamberlain 2014). In order to study correlations between

the rates of evolution of each character, we fitted a set of evolutionary variance covariance matrices (Revell and Collar 2009) (R phytools::evol.vcv). When fitting all covariance terms simultaneously, we selected the largest set of characters that would allow the analysis to run without computational singularities. This excluded many of the morphometric characters which are linearly dependent on other characters. Since the functions do not tolerate missing data, we ran the analyses in two ways: One including all taxa but transforming absent states to zeroes, and another removing the taxa with absent states. To test whether phenotypic integration changes across selective regimes determined by the reconstructed feeding guilds, we carried out character-pairwise variance covariance analysis comparing alternative models (R phytools::evolvcv.lite) such as models where correlations are the same across the whole tree and models where correlations differ between selective regimes. These analyses could only be carried out on the subset of taxa for which diet data is available, and only among character pairs that are not computationally singular for that taxonomic subset. Finally, we compared regime-specific variance covariance matrices to the general matrix and to their preceding regime matrix to identify the changes in character dependence unique to each regime (see Appendix 20). Gelatinous specialist correlations could only be estimated for a small subset of characters present in *Apolemia*.

To test how many times extreme nematocyst morphologies evolved, we reconstructed the ancestral states of $\log(\text{length}/\text{width})$ of the different nematocyst types, and identified the branches with the greatest shifts. In addition to characterizing the shifts in the state values of haploneme and heteroneme elongation, we identified and located regime shifts for the rate of evolution using a Bayesian Analysis of Macroevolutionary Mixtures (BAMM) (Rabosky et al. 2014) (Appendix 16).

Results

Phylogeny – Only 5 nodes in the unconstrained inference were incongruent with the (Munro et al. 2018) transcriptome tree. The topology of the constrained tree presented here (Fig. 4)

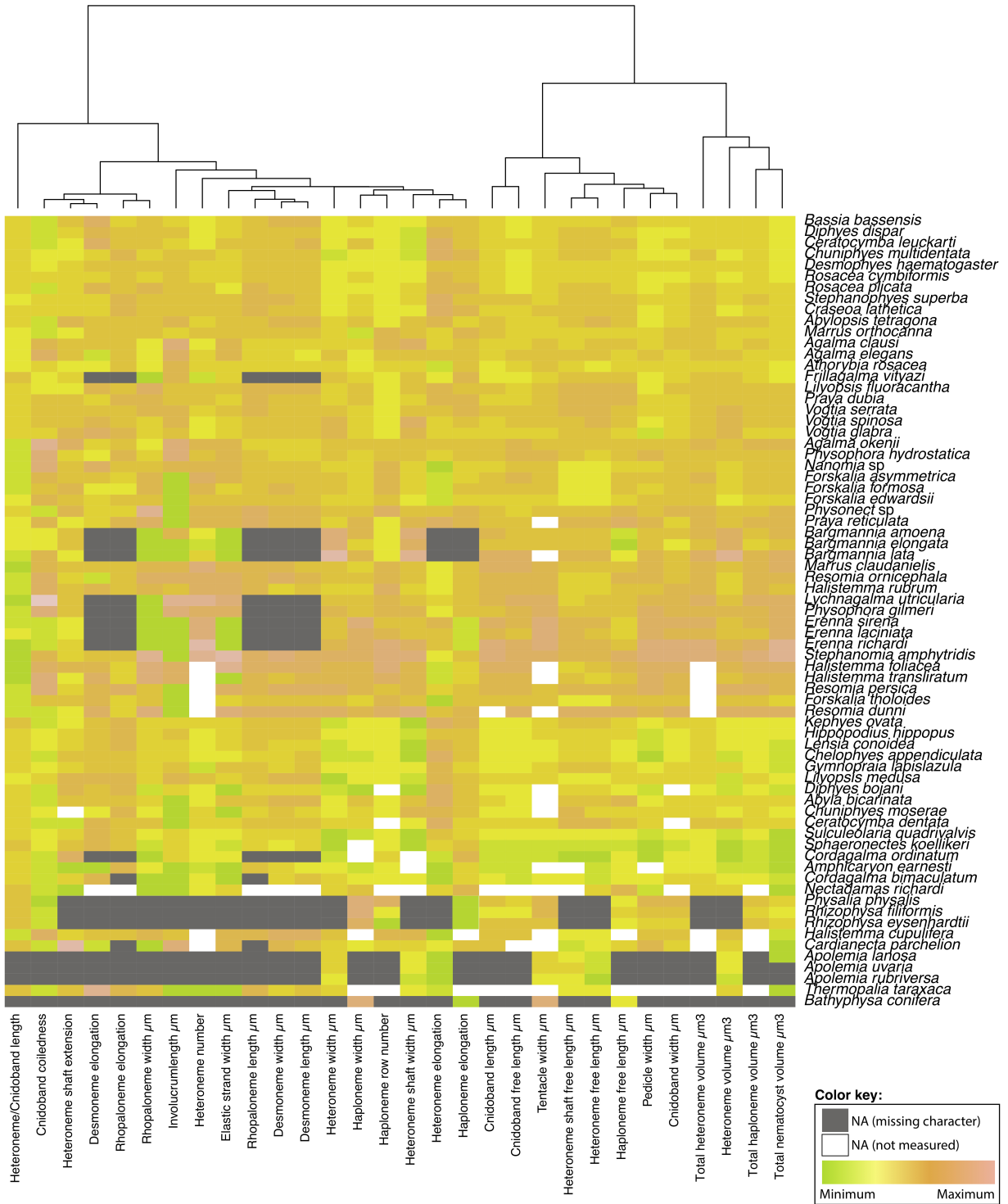


Figure 3: Heatmap summarizing the morphological diversity measured for 96 species of siphonophores clustered by similarity (raw data in Appendix 3). Missing values from absent characters presented as dark grey cells, missing values produced from technical difficulties presented as white cells. Values scaled by character.

³⁰¹ is congruent with the resolved nodes in (Dunn et al. 2005) and (Munro et al. 2018).

³⁰² We retained the clade nomenclature defined in (Dunn et al. 2005) and (Munro et al.
³⁰³ 2018), such as Codonophora to indicate the sister group to Cystonectae, Euphysonectae to
³⁰⁴ indicate the sister group to Calycophorae, Clade A and B to indicate the two main lineages
³⁰⁵ within Euphysonectae. In addition, we define two new clades within Codonophora (Fig. 4):
³⁰⁶ Eucladophora as the clade containing *Agalma elegans* and all taxa that are more closely related
³⁰⁷ to it than to *Apolemia lanosa*, and Tendiculophora as the clade containing *Agalma elegans* and
³⁰⁸ all taxa more closely related to it than to *Bargmannia elongata*. Eucladophora is characterized
³⁰⁹ by bearing spatially differentiated tentilla with proximal heteronemes and a narrower terminal
³¹⁰ filament region. The etymology derives from the Greek *eu+kládos+phóros* for “true branch
³¹¹ bearers”. Tendiculophora are characterized by bearing rhopalonemes and desmonemes in the
³¹² terminal filament, having a pair of elastic strands, and developing proximally detachable
³¹³ cnidobands. The etymology of this clade is derived from the Latin *tendicula* for “snare or
³¹⁴ noose” and the Greek *phóros* for “carriers”.

³¹⁵ *Evolutionary dynamics between diet and tentillum morphology* – The reconstructions of
³¹⁶ feeding guilds show that generalism is not likely to be ancestral, and it appears to have evolved
³¹⁷ at least two times independently (Fig. 5). Generalism evolves twice independently from
³¹⁸ large crustacean specialist lineages, supporting hypothesis 3. Feeding guild specializations
³¹⁹ have shifted from an alternative ancestral state at least five times, supporting hypothesis
³²⁰ 2. Individual prey type presence reconstructions show that copepod specialization and fish
³²¹ specialization evolved twice, ostracod specialization evolved at least once. The OUwie model
³²² comparison shows that out of 30 characters, 10 show significantly stronger support for the
³²³ diet-driven multi-optima multi-rate OU model (Appendix 14). These characters include
³²⁴ terminal filament nematocyst size and shape, involucrum length, elastic strand width, and
³²⁵ heteroneme number. Most of these characters are found exclusively in Tendiculophora,
³²⁶ thus this reflects processes that could be unique to this subtree. Five characters including
³²⁷ cnidoband length, cnidoband shape, and haploneme length show maximal support for a

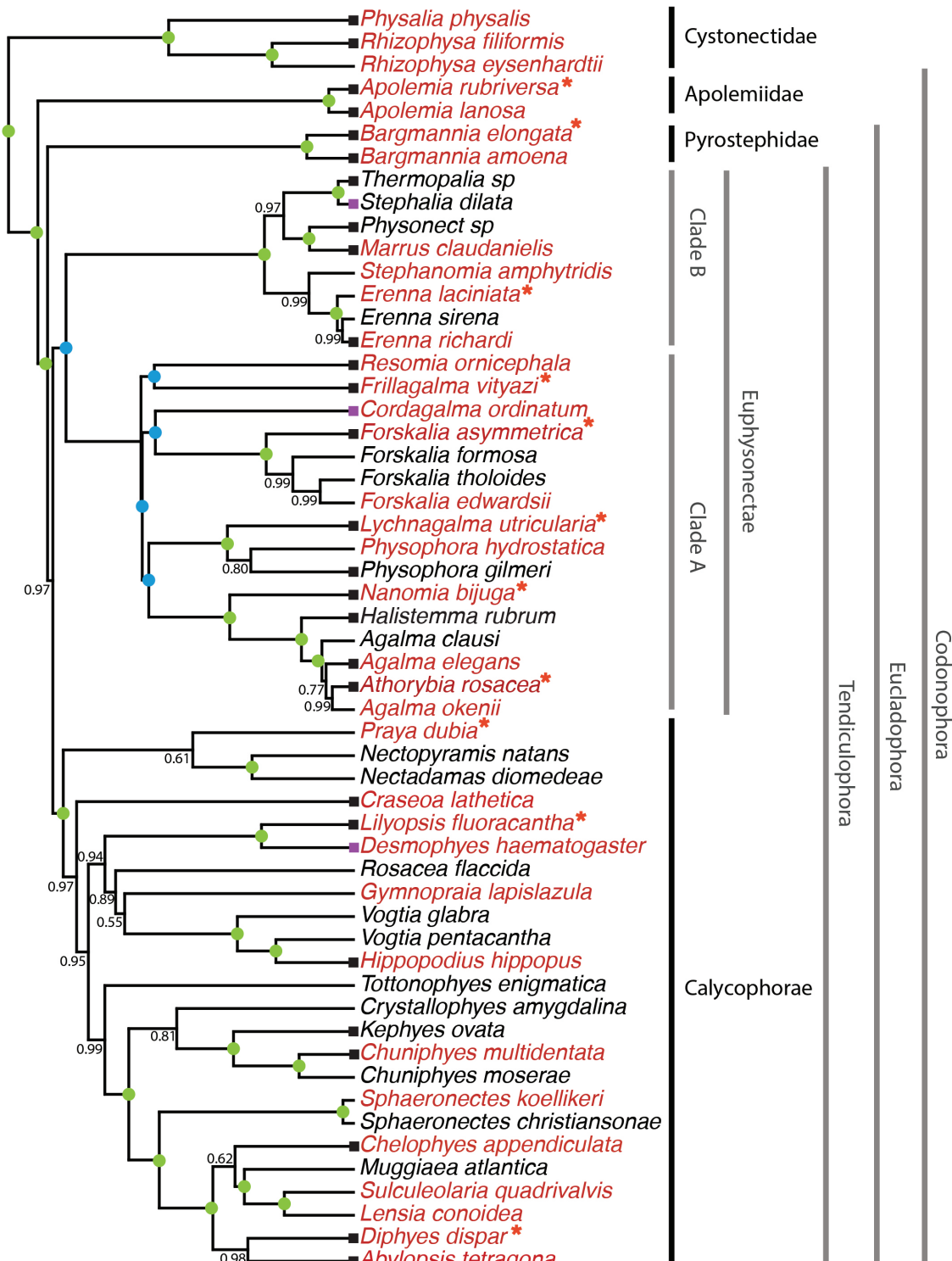


Figure 4: Bayesian time-tree built from 18S + 16S concatenated sequences. Branch lengths estimated using relaxed molecular clock. Species names in red indicate replicated representation in the morphology data. Species marked with an asterisk were recorded using high speed video. Nodes labeled with bayesian posteriors (BP). Green circles indicate BP = 1. Blue circles indicate nodes constrained to be congruent with (Munro *et al.* 2018). Tips with black squares indicate the species with transcriptomes used in (Munro *et al.* 2018). Tips with grey squares indicate genus-level correspondence to taxa included in (Munro *et al.* 2018). The tree includes all the data available for the analysis, including species from Munro *et al.* 2018 and new data from this study.

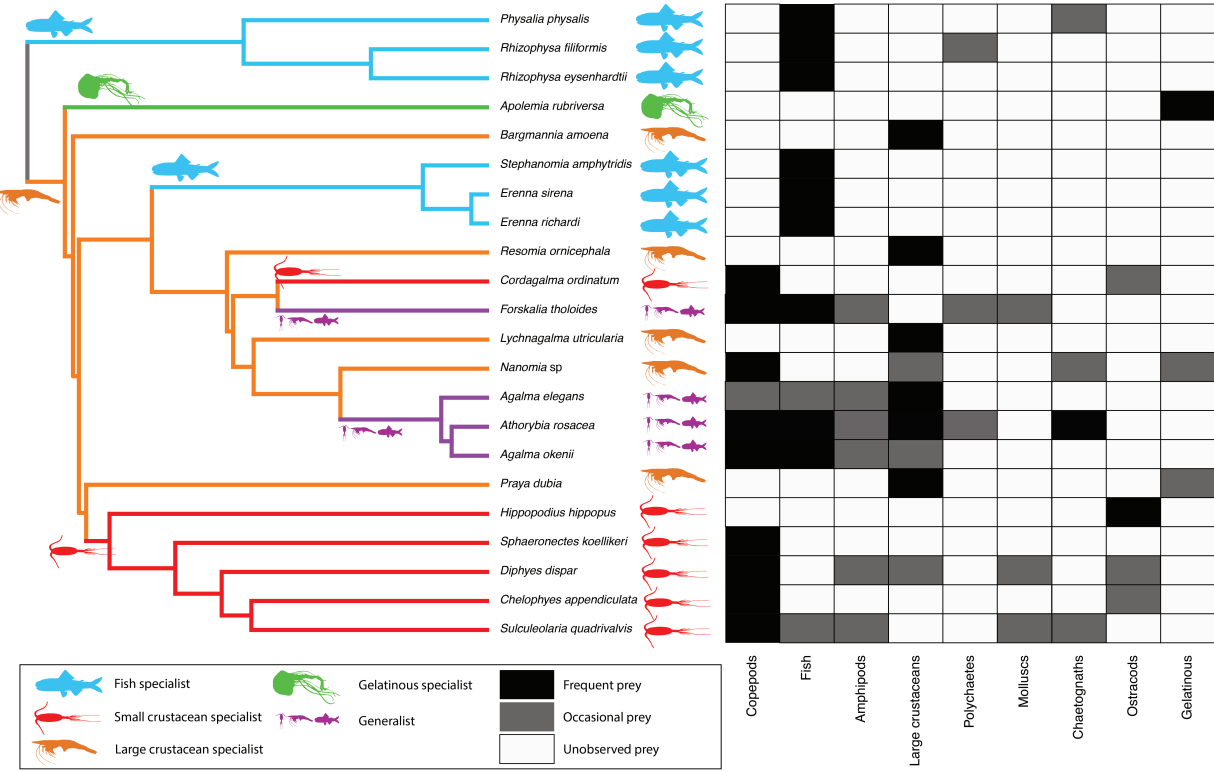


Figure 5: Left - Subset phylogeny showing the mapped feeding guild regimes that were used to inform the *OUwie* analyses. Right - Grid showing the prey items consumed from which the feeding guild categories were derived. Diet data were obtained from the literature review in Appendix 10.

328 diet-driven single-optimum OU model. The remaining 15 characters support BM (or OU
 329 with marginal AICc difference with BM).

330 Phylogenetic logistic regressions identified evolutionary associations between individual
 331 characters and the presence of particular prey types in the diet (Fig. 5, right). Shifts toward
 332 ostracod presence in diet correlated with reductions in pedicle width and total haploneme
 333 volume. Shifts to copepod presence in the diet were associated with reductions in haploneme
 334 width, cnidoband length and width, total haploneme and heteroneme volumes, and tentacle
 335 and pedicle widths. Consistently, transitions to decapod presence in the diet correlated with
 336 more coiled cnidobands (Appendix 17).

337 Phylogenetic regressions of continuous characters against prey selectivity data produced
 338 additional insights. Fish selectivity is associated with increased number of heteronemes

339 per tentillum, increased roundness of nematocysts (desmonemes and haplonemes), larger
 340 heteronemes, reduced heteroneme/cnidoband length ratios, smaller rhopalonemes, lower
 341 haploneme SA/V ratios, and increased size of the cnidoband, elastic strand, pedicle and
 342 tentacle widths. Decapod-selective diets were associated with increasing cnidoband size and
 343 coiledness, haploneme row number, elastic strand width, and heteroneme number. Copepod-
 344 selective diets evolved in association with smaller heteroneme and total nematocyst volumes,
 345 smaller cnidobands, rounder rhopalonemes, elongated heteronemes, narrower haplonemes
 346 with higher SA/V ratios, and smaller heteronemes, tentacles, pedicles and elastic strands.
 347 Selectivity for ostracods was associated with reductions in size and number of heteroneme
 348 nematocysts, reductions in cnidoband size, number of haploneme rows, heteroneme number,
 349 and cnidoband coiledness. Heteroneme length and shape also correlated negatively with
 350 chaetognath selectivity.

351 When some of the diet-morphology associations reported in the literature (Purcell 1984;
 352 Purcell and Mills 1988) were tested for correlated evolution (Table 1), we found that most
 353 were consistent with an evolutionary explanation except the relationship between terminal
 354 filament nematocysts (rhopalonemes and desmonemes) and crustaceans in the diet. The latter
 355 is likely a product of the larger species richness of crustacean-eating species with terminal
 356 filament nematocysts, rather than simultaneous evolutionary gains.

357 Table 1. Tests of correlated evolution between morphological characters and aspects of
 358 the diet found correlated in the literature.

Character	Aspect of diet	Test of evolutionary association	Relationship sign	P-value	Number of taxa	Association first report
Differentiated cnidobands	Hard bodied prey	Page's test	+	0.017	19	Purcell, 1984
Heteroneme volume	Copepod prey size	pGLS	+	0.002	8	Purcell, 1984
Terminal filament nematocysts	Crustacean diet	Page's test	+	0.200	19	Purcell & Mills, 1988
Number of nematocyst types	Soft-bodied prey	Phylogenetic logistic regression	-	0.040	22	Purcell & Mills, 1988

359

360

361 *Generating dietary hypotheses using tentillum morphology* – The discriminant analysis of
 362 principal components for feeding guild (7 principal components, 4 discriminants) produced
 363 100% discrimination, and the highest loading contributions were found for the characters

364 (ordered from highest to lowest): Involucrum length, heteroneme volume, heteroneme number,
 365 total heteroneme volume, tentacle width, heteroneme length, total nematocyst volume, and
 366 heteroneme width (Appendix 15.1). We used the predictions from this discriminant function
 367 to generate hypotheses about the feeding guild of 45 species in our morphological data (Fig.
 368 @figure6)). This projection predicts that two other *Apolemia* species may also be gelatinous
 369 prey specialists like *Apolemia rubriversa*, and that *Erenna laciniata* may be a fish specialist
 370 like *Erenna richardi*.

371 Table 2. Discriminant analysis of principal components for the presence of specific prey
 372 types using the morphological data. Top quartile variable (character) contributions to the
 373 linear discriminants are ordered from highest to lowest. Logistic regressions and GLMs were
 374 fitted to predict prey type presence and selectivity respectively. The sign of the slope of each
 375 predictor is reported, and highlighted green if significant (p value < 0.05). Pseudo- R^2 (%)
 376 approximates the percent variance explained by the model.

Prey type	DAPC	GLM for prey type presence (22 taxa)		Best fitting GLM for prey type selectivity (Purcell, 1981) (7 taxa)	
		Discrimination (%)	Top quartile variable contributions	Sign	Pseudo- R^2 (%)
Copepods	95.4	Total nematocyst volume	-	-	
		Tentacle width	-	+	
		Haploneme elongation	-	+	
		Haploneme surface area/volume ratio	+	-	
		Haploneme row number	+	+	
		Cnidoband length	-	+	
		Cnidoband width	-	-	
Fish	68.1	Cnidoband free length	+	+	
		Total haploneme volume	-	+	
		Heteroneme volume	+	-	
		Total nematocyst volume	-	+	
		Total heteroneme volume	-	-	
		Cnidoband length	-	-	
		Cnidoband free length	+	+	
Large crustaceans	81.8	Involucrum length	-	-	
		Pedicle width	+	+	
		Involucrum length	+	+	
		Total heteroneme volume	-	-	
		Elastic strand width	-	+	
		Rhopaloneme length	+	+	
		Heteroneme volume	+	-	

377

378 When predicting soft and hard bodied prey specialization, the DAPC achieved 90.9%
 379 discrimination success, only marginally confounding hard-bodied specialists with generalists
 380 (Appendix 15.4). The main characters driving the discrimination are involucrum length,
 381 heteroneme number, heteroneme volume, tentacle width, total nematocyst volume, total

382 haploneme volume, elastic strand width, and heteroneme length. Discriminant analyses and
383 GLM logistic regressions were also applied to specific prey type presence and selectivity
384 (Table 2), revealing the sign of their predictive relationship to each prey type. We only
385 selected prey types with sufficient variation in the data to carry out these analyses (copepods,
386 fish, and large crustaceans). While the presence of fish or large crustaceans in the diet cannot
387 be unambiguously discriminated using tentillum morphology (Appendix 15), specialization
388 on fish or large crustacean prey can be fully disentangled (Appendix 15.1). For each prey
389 type studied, tentilla morphology is a much better predictor of prey selectivity than of
390 prey presence, despite prey selectivity data being available for a smaller subset of species.
391 Interestingly, many of the morphological predictors had opposite slope signs when predicting
392 prey selectivity *versus* predicting prey presence in the diet (Table 2).

393 *Evolution of tentillum and nematocyst characters* – One third of the characters measured
394 support a non-phylogenetic generative model, indicating they are not likely to be phylogeneti-
395 cally distributed (Appendix 12). Total nematocyst volume and cnidoband-to-heteroneme
396 length ratio showed strongly conserved phylogenetic signals. 74% of characters present a
397 significant phylogenetic signal, yet only total nematocyst volume, haploneme length, and
398 heteroneme-to-cnidoband length ratio had a phylogenetic signal $K > 1$. 67% of characters
399 support BM models, indicating a history of neutral constant divergence. No relationship
400 between phylogenetic signal and BM model support was found. Haploneme nematocyst
401 length is the only character with support for an EB model of decreasing rate of evolution
402 with time. No character had support for a single-optimum OU model (when uninformed by
403 feeding guild regime priors).

404 The phylogenetic positions of the main categorical character shifts were reconstructed
405 using stochastic character mappings (Appendix 18), and summarized in Figure 7. Haploneme
406 nematocysts are likely ancestrally present in the tentacles, since they are present in the
407 tentacles of many other hydrozoans. Haplonemes diverged into spherical isorhizas of 2
408 size classes in Cystonectae, and elongated anisorhizas of one size class in Codonophora.

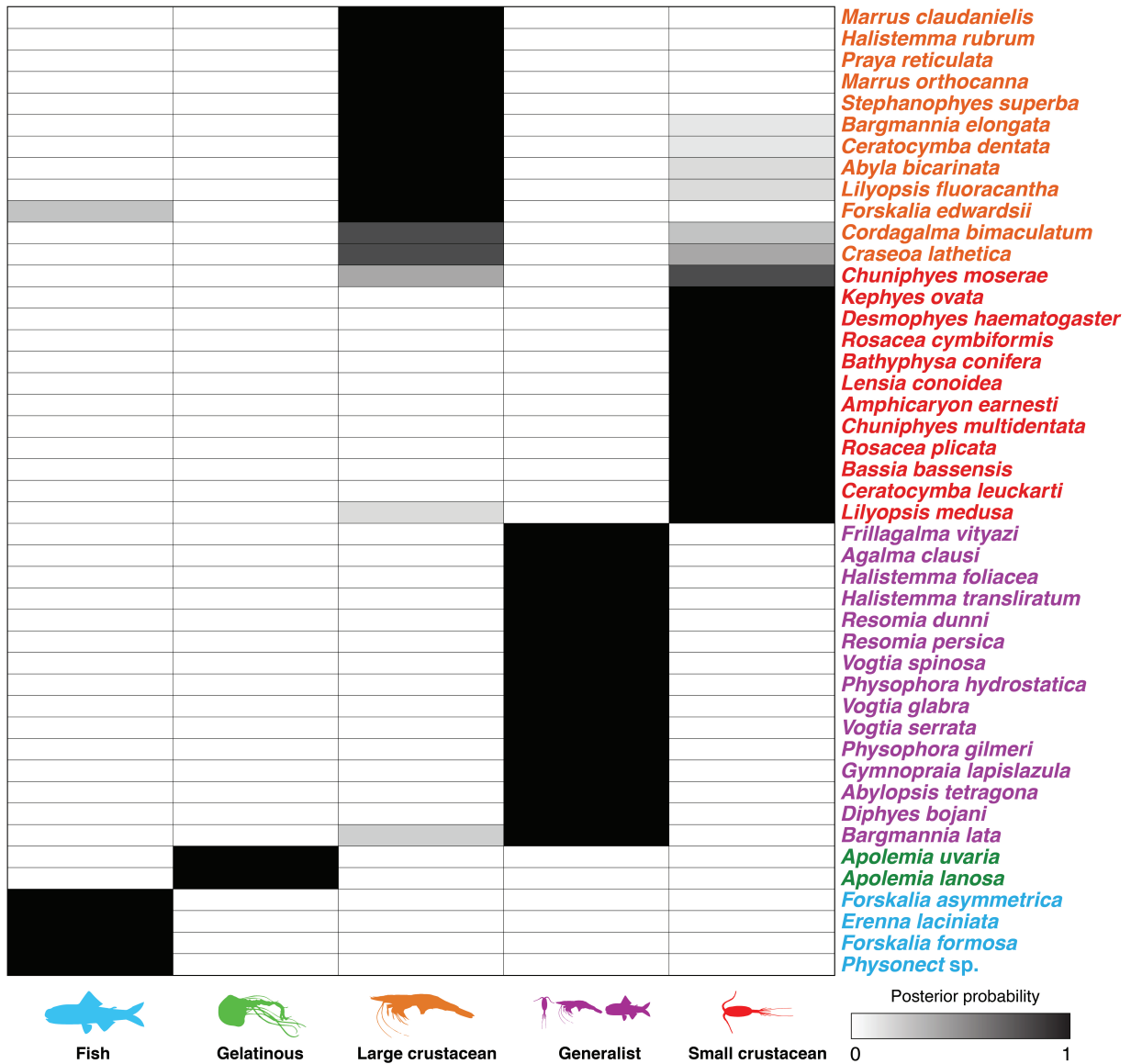


Figure 6: Hypothetical feeding guilds for siphonophore species predicted by a 6 PCA DAPC (in Appendix 15.1). Cell darkness indicates posterior probability of belonging to each guild. Training data set transformed so inapplicable states are computed as zeroes. Species ordered and colored according to their predicted feeding guild.

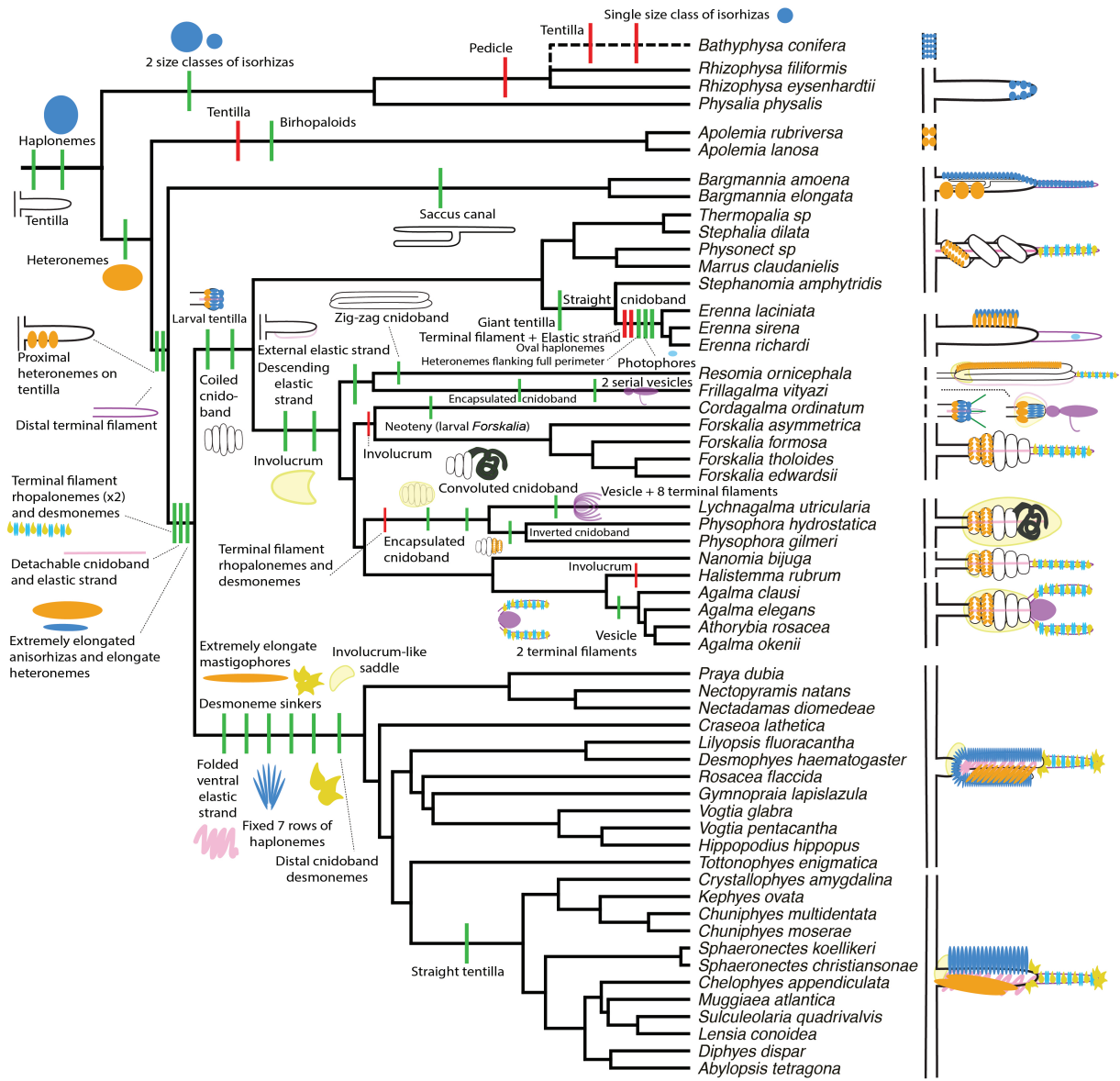


Figure 7: Siphonophore cladogram with the main categorical character gains (green) and losses (red) mapped. Some branch lengths were modified from the Bayesian chronogram to improve readability. The main visually distinguishable tentillum types are sketched next to the species that bear them, showing the location and arrangement of the main characters. In large complex-shaped tentilla, haplonemes were omitted for simplification. The rhizophysid *Bathyphysa conifera* branch was appended manually as a polytomy (dashed line).

⁴⁰⁹ Haplonemes were likely lost in the tentacles of *Apolemia*, but spherical isorhizas are retained
⁴¹⁰ in other *Apolemia* tissues (Siebert et al. 2013). Similarly, while heteronemes exist in other
⁴¹¹ tissues of cystonects, they only appear in the tentacles of codonophorans as birhopaloids in
⁴¹² *Apolemia*, ancestral stenoteles in eucladophoran physonects, and microbasic mastigophores in
⁴¹³ calycophorans.

⁴¹⁴ Eucladophora (the clade containing Pyrostephidae, Euphysonectae, and Calycophorae,
⁴¹⁵ see Fig. 4) encompasses most of the extant Siphonophore species (178 of 186). Innovations
⁴¹⁶ evolved in the stem of this group include spatially segregated heteroneme and haploneme
⁴¹⁷ nematocysts, terminal filaments, and elastic strands (Fig. 7). Pyrostephids evolved a unique
⁴¹⁸ bifurcation of the axial gastrovascular canal of the tentillum known as the “saccus” (Totton
⁴¹⁹ and Bargmann 1965). The stem to the clade Tendiculophora (clade containing Euphysonectae
⁴²⁰ and Calycophorae, see Fig. 4) subsequently acquired further novelties such as the desmoneme
⁴²¹ and rhopaloneme (acrophore subtype ancestral) nematocysts on the terminal filament (Fig.
⁴²² 7), which bear no other nematocyst type (Fig. 1). These are arranged in sets of 2 parallel
⁴²³ rhopalonemes for each single desmoneme (Skaer 1988, 1991). The involucrum is an expansion
⁴²⁴ of the epidermal layer that can cover part or all of the cnidoband (Fig. 2). This structure,
⁴²⁵ together with differentiated larval tentilla, appeared in the stem branch to Clade A physonects.
⁴²⁶ Calycophorans evolved unique novelties such as larger desmonemes at the distal end of the
⁴²⁷ cnidoband, pleated pedicles with a “hood” (here considered homologous to the involucrum) at
⁴²⁸ the proximal end of the tentillum, anacrophore rhopalonemes, and microbasic mastigophore-
⁴²⁹ type heteronemes. While calycophorans have diversified into most of the extant described
⁴³⁰ siphonophore species (108 of 186), their tentilla have not undergone any major categorical
⁴³¹ gains or losses since their most recent common ancestor. Nonetheless, they have spreaded
⁴³² over a broad span of variation in nematocyst and cnidoband sizes.

⁴³³ *Phenotypic integration of the tentillum* – The quantitative characters we measured from
⁴³⁴ tentilla and their nematocysts are highly correlated. The results indicate that the dimen-
⁴³⁵ sionality of tentillum morphology is low, that many traits are associated with size, but that

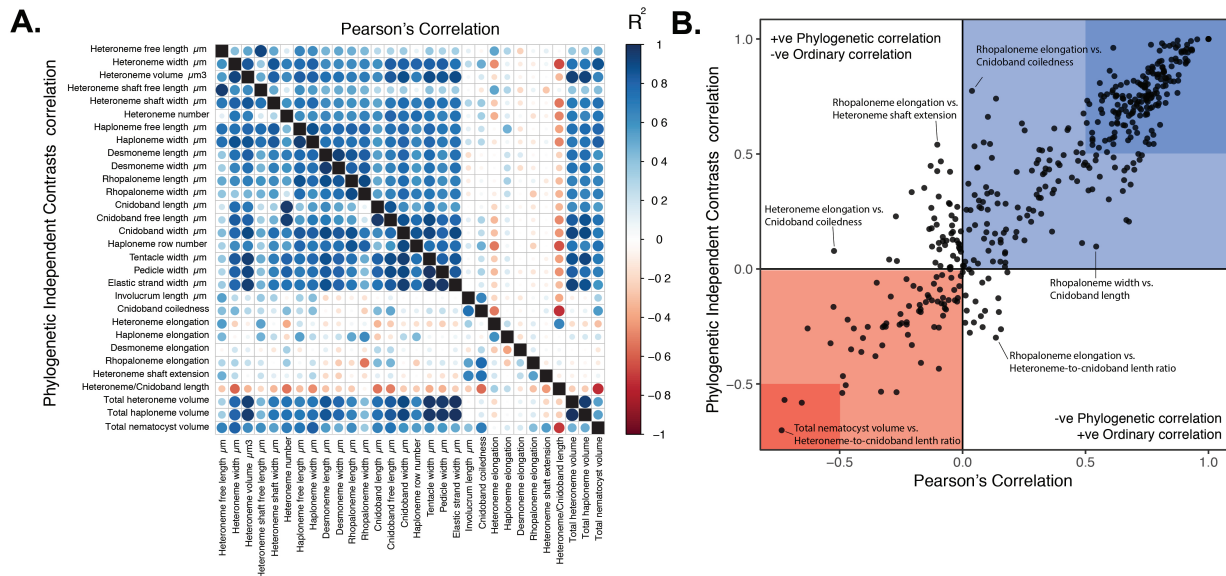


Figure 8: A. Correlogram showing strength of ordinary (upper triangle) and phylogenetic (lower triangle) correlations between characters. Both size and color of the circles indicate the strength of the correlation (R^2). B. Scatterplot of phylogenetic correlation against ordinary correlation showing a strong linear relationship ($R^2 = 0.92$, 95% confidence between 0.90 and 0.93). Light red and blue boxes indicate congruent negative and positive correlations respectively. Darker red and blue boxes indicate strong (<-0.5 or >0.5) negative and positive correlation coefficients respectively.

436 nematocyst arrangement and shape are independent of it. Of the phylogenetic correlations
437 (Fig. 8a, lower triangle), 81.3% were positive and 18.7% were negative, while of the ordinary
438 correlations (Fig. 8a, upper triangle) 74.6% were positive and 25.4% were negative. Half
439 (49.9%) of phylogenetic correlations were >0.5 , while only 3.6% are < -0.5 . Similarly, of
440 the across-species correlations, 49.1% were >0.5 and only 1.5% were < -0.5 . 13.9% of char-
441 acter pairs had opposing phylogenetic and ordinary correlation coefficients. Just 4% have
442 negative phylogenetic and positive ordinary correlations (such as rhopaloneme elongation ~
443 heteroneme-to-cnidoband length ratio and haploneme elongation, or haploneme elongation
444 ~ heteroneme number), and vice versa for 9.9% of character pairs (such as heteroneme
445 elongation ~ cnidoband convolution and involucrum length, or rhopaloneme elongation with
446 cnidoband length). These disparities can be caused by Simpson's paradox (Blyth 1972), the
447 reversal of the sign of a relationship when a third variable (or a phylogenetic topology (Uyeda
448 et al. 2018)) is considered. However, no character pair had correlation coefficient differences
449 larger than 0.64 between ordinary and phylogenetic correlations (heteroneme shaft extension
450 ~ rhopaloneme elongation has a Pearson's correlation of 0.10 and a phylogenetic correlation of
451 -0.54). Rhopaloneme shape shows the most incongruences between phylogenetic and ordinary
452 correlations with other characters.

453 The variance covariance matrices (Appendix 20.1-20.2) are congruent with the abundant
454 positive correlations observed among simple measurement characters in Fig. 8a. However, this
455 analysis reveals more clearly the diagonal blocks that constitute the integration modules, such
456 as the heteroneme block, the terminal filament nematocyst block, and the cnidoband-pedicle-
457 tentacle block. These results were not very sensitive to transformation of inapplicable states
458 and taxon sampling. When we compared the rate covariance terms between characters across
459 the different feeding guild regimes (Appendix 20.4), we found that half (48%) of the character
460 pairs presented different correlation coefficients across different regimes, indicating that the
461 mode of phenotypic integration may also shift with trophic niche. When contrasting the
462 regime-specific rate correlation matrices to the whole-tree matrix, we were able to identify the

463 character dependencies that are unique to each predatory niche (Appendix 20.6). Similarly,
464 when we contrasted these matrices to the large crustacean (ancestral) matrix, we identified
465 the main shifts in character dependencies associated to regime shifts.

466 Under the majority of SIMMAP outcomes, large crustaceans specialists are the first regime
467 to appear, and other regimes evolve in a shift from this ancestral specialization. Compared
468 to the rate correlation matrix estimated over the whole tree, large crustacean specialists
469 present strong negative correlations between haploneme elongation and heteroneme size, and
470 between rhopaloneme shape and tentillum size, as well as with involucrum length. With
471 the appearance of generalists (*Forskalia* and Agalmatids), terminal filament nematocyst
472 (desmonemes and rhopalonemes) sizes become negatively correlated with the sizes of most
473 characters. In addition, heteroneme and rhopaloneme elongation became positively correlated
474 with cnidoband size. When large crustacean specialists switched to small crustacean prey in
475 *Cordagalma* and calycophorans, haploneme size became inversely correlated with heteroneme
476 elongation, which developed a strong positive relationship with tentillum size. Simultaneously,
477 in these small crustacean specialists, haploneme elongation became positively correlated with
478 heteroneme size. With the evolution of fish prey specialization in cystonects and within
479 Clade B, haploneme elongation became negatively correlated with heteroneme elongation
480 (in Clade B), and the surface area to volume ratio of haploneme nematocysts switched
481 from the strong negative relationship with cnidoband size found in every other regime to a
482 positively correlation. Gelatinous specialization, albeit appearing only once, also carries a
483 unique signature in character rate correlation shifts, with an increase in the strength of the
484 correlation between heteroneme shape and shaft width, consistent with the appearance of
485 birrhopaloid nematocysts with swollen shafts that are effective at anchoring gelatinous tissue.

486 In the non-phylogenetic PCA morphospace using only simple characters (Fig. 9), PC1
487 (aligned with tentillum and tentacle size) explained 69.3% of the variation in the tentillum
488 morphospace, whereas PC2 (aligned with heteroneme length, heteroneme number, and
489 haploneme arrangement) explained 13.5%. In a phylogenetic PCA, 63% of the evolutionary

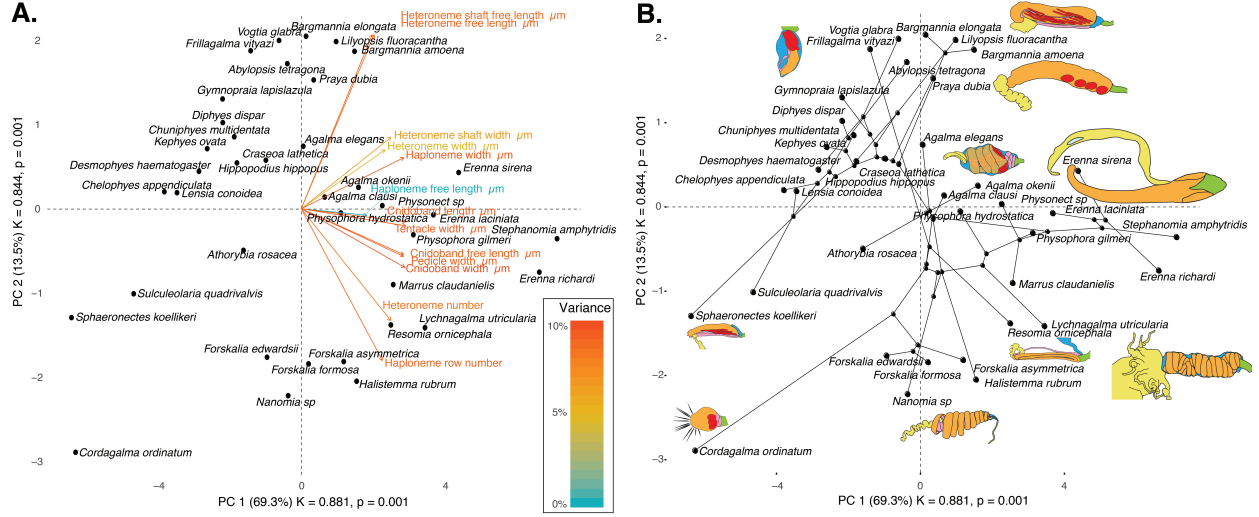


Figure 9: Phylogenomorphospace of the simple continuous characters principal components, excluding ratios and composite characters. A. Variance explained by each variable in the PC1-PC2 plane. Axis labels include the phylogenetic signal (K) for each component and p-value. B. Phylogenetic relationships between the species points distributed in that same space.

variation in the morphospace is explained by PC1 (aligned with shifts in tentillum size), while 18% is explained by PC2 (aligned with shifts in heteroneme number and involucrum length).

Evolution of nematocyst shape – Haploneme nematocyst evolution has been mainly

driven by a single large shift towards elongation in Tendiculophora, which contains the majority of described siphonophore species. There is one secondary return to more oval, less elongated haplonemes in *Erenna*, but it does not reach the sphericity present in Cystonectae or Pyrostephidae (Fig. 10). Heteroneme evolution presents a less radical evolutionary history, where Tendiculophora evolved more elongate heteronemes, but the difference between theirs and other siphonophores is much smaller than the variation in shape within Tendiculophora, bearing no phylogenetic signal. In this group, the evolution of heteroneme shape has diverged in both directions, and there is no correlation with haploneme shape, which has remained fairly constant (elongation between 1.5 and 2.5).

Haploneeme and heteroneme shape share 21% of their variance across extant values, and

53% of variance in their shifts along the branches of the phylogeny. However, much of this correlation is due to the contrast between Pyrostephidae and their sister group Tendiculophora

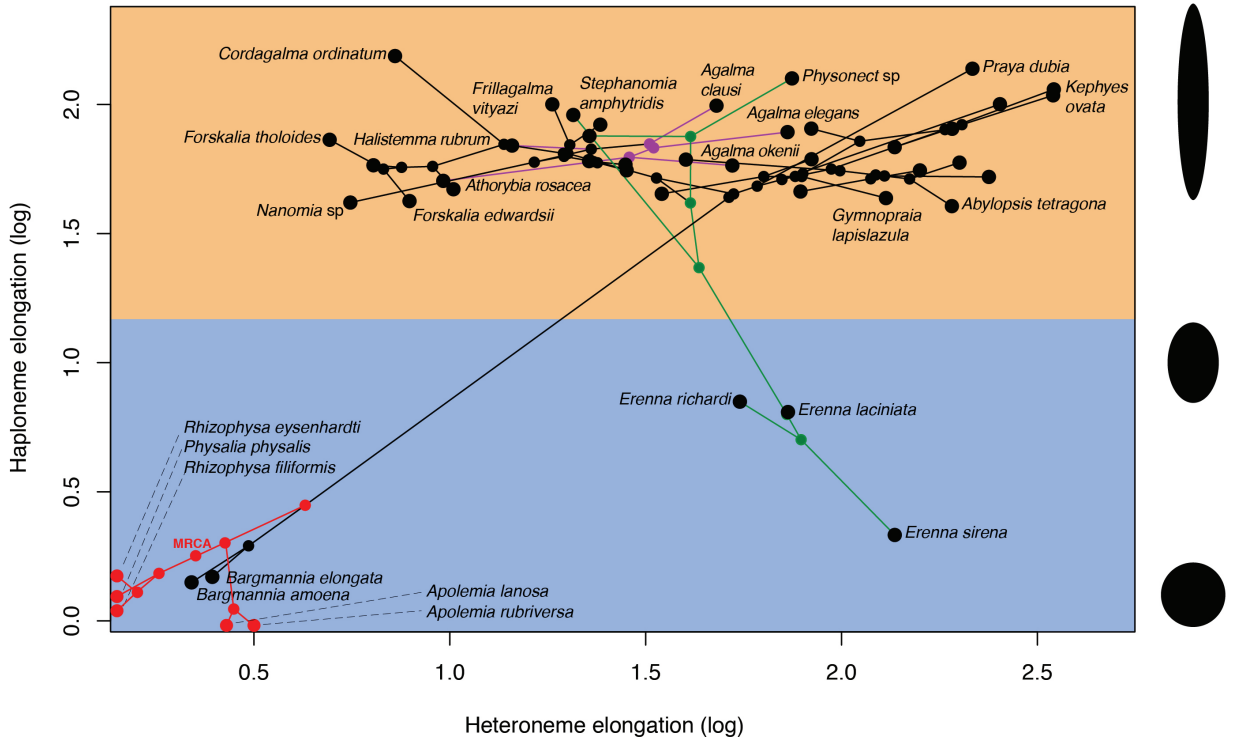


Figure 10: Phylomorphospace showing haploneme and heteroneme elongation (log scaled). Orange area delimits rod-shaped haplonemes, blue area covers oval and round shaped haplonemes. Smaller dots and lines represent phylogenetic relationships and ancestral states of internal nodes under BM. Species nodes in red were manually added to the plot. Cystonects have no tentacle heteronemes and are projected onto the haploneme axis. Apolemids have no tentacle haplonemes and are projected onto the heteroneme axis. Colored branches and nodes correspond to BAMM regimes of accelerated haploneme shape (green) and heteroneme shape (violet) evolution.

505 (Fig. 4). BAMM identified a regime shift in heteroneme shape evolution on the branches
506 leading to *Agalma* and *Athorybia*. For the rates of haploneme shape evolution, BAMM
507 identified two main independent regime shifts (Fig. 10): one in the branch leading to
508 Codonophora (anisorhizas diverging from cystonects' spherical isorhizas), and one in the
509 branch leading to Clade B physonects. Clade B includes *Erenna*, *Stephanomia*, *Marrus*, and
510 rhodaliids. Most of these taxa have rod-shaped anisorhizas, but *Erenna* has oval ones). No
511 clear regime shift patterns were identified in the evolution of desmoneme and rhopaloneme
512 shape.

513 *Functional morphology of tentillum and nematocyst discharge* – Tentillum and nematocyst
514 discharge high speed measurements are available in Appendix 4. While the sample sizes of
515 these measurements were insufficient to draw reliable statistical results at a phylogenetic level,
516 we did observe patterns that may be relevant to their functional morphology. For example,
517 cnidoband length is strongly correlated with discharge speed (p value = 0.0002). This is
518 probably the sole driver of the considerable difference between euphysonect and calycophoran
519 tentilla discharge speeds (average discharge speeds: 225.0mm/s and 41.8mm/s respectively;
520 t-test p value = 0.011), since the euphysonects have larger tentilla than the calycophorans
521 among the species recorded.

522 We also observed that calycophoran haploneme tubules fire faster than those of eu-
523 physonects (T-test p value = 0.001). Haploneme nematocysts discharge 2.8x faster than
524 heteroneme nematocysts (T-test p value = 0.0012). Finally, we observed that the stenoteles
525 of the Euphysonectae discharge a helical filament that “drills” itself through the medium it
526 penetrates as it everts.

527 Discussion

528 The core aims of this study are to examine the evolutionary history of siphonophore tentilla and
529 diet, characterize the evolutionary shifts in their trophic niches, and identify the morphological
530 characters that evolve with changes in prey type. We inquire whether the relationships between

531 form and function observed in extant taxa are due to correlated evolution or non-evolutionary
532 causes, whether the evolution of their trophic specializations supports or challenges traditional
533 ecological theory (such as the idea specialists evolve from generalists), and whether the diets
534 of siphonophores can be hypothesized by observing their tentacles. In addition, we produced
535 novel findings on tentillum morphology, siphonophore phylogeny, nematocyst character
536 evolution, and tentillum discharge dynamics.

537 *Evolution of tentillum morphology with diet* – Siphonophores are an abundant group of
538 zooplankton in oceanic ecosystems (Longhurst 1985; O’Brien 2007). While little is known
539 about siphonophore trophic ecology, what is known indicates that they occupy a central
540 position in midwater food webs (Choy et al. 2017), serving as trophic intermediaries between
541 smaller zooplankton and higher trophic level predators. Siphonophore species have been
542 observed to feed on a variety of prey with very different sizes, traits, and behaviors. Because
543 there is a total absence of siphonophores in the fossil record, how they became established
544 as the ubiquitous and diversified predators in today’s oceans remains an open question.
545 Predators that use similar tools for prey capture tend to capture similar prey, so their
546 abundance and coexisting species diversity are inversely related due to competitive exclusion
547 by resource limitation (Schluter 2000). However, this is not consistent with what we observe
548 in siphonophores, which have been found to be both very abundant and locally diverse
549 (Longhurst 1985, @mapstone2014global). We hypothesize that siphonophores have escaped
550 this by specializing on different prey resources.

551 According to our reconstructions, the evolutionary history of siphonophore diets indicates
552 that being a specialist was an ancestral aspect of their trophic niche, while trophic generalism
553 is likely a derived condition. Several studies (reviewed in (Futuyma and Moreno 1988))
554 have suggested that resource specialization is an irreversible dead end due to the constraints
555 posed by phenotypic specialization. Our reconstructions show that this is not the case for
556 siphonophores, where the prey type on which they specialize has shifted at least 5 times, and
557 generalism has evolved independently at least twice. Among the evolutionary hypotheses

558 considered, we find support for both hypotheses 2 (specialist resource switching) and 3
559 (specialist to generalist), but no support for hypothesis 1 (generalist to specialist). The
560 evolutionary history of tentilla shows that siphonophores are an example of trophic niche
561 diversification via morphological innovation and evolution, which allowed transitions between
562 specialized trophic niches. This strategy is particularly important in a deep open ocean
563 ecosystem, which is a relatively homogeneous physical environment, where the primary niche
564 heterogeneity available is the potential interactions between organisms (Robison 2004).

565 One of the most common prey items found in siphonophore diets is copepods (Fig. 5).
566 Copepod-specialized diets have evolved convergently in *Cordagalma* and some Calycophorans.
567 These evolutionary transitions happened together with transitions to smaller tentilla with
568 fewer cnidoband nematocysts. Tentilla are expensive single-use structures, therefore we would
569 expect that specialization in small prey would beget reductions in the size of the prey capture
570 apparatus to the minimum required for the ecological function. *Cordagalma*'s tentilla strongly
571 resemble the larval tentilla (only found in the first-budded feeding body of the colony) of
572 their sister genus *Forskalia* spp. This indicates that the evolution of *Cordagalma* tentilla
573 could be a case of paedomorphosis associated with predatory specialization.

574 (Purcell 1984) showed that haplonemes have a penetrating function as isorhizas in
575 cystonects and an adhesive function as anisorhizas in Tendiculophora. The two clades that
576 have been observed primarily feeding on fish (Cystonectae and Clade B, which includes
577 *Erenna*, *Stephanomia*, *Marrus*, and rhodaliids) present an accelerated rate of haploneme
578 shape evolution towards more compact haplonemes, significantly distinct from their closest
579 relatives. Isorhizas in cystonects are known to penetrate the skin of fish during prey capture,
580 and to deliver the toxins that aid in paralysis and digestion (Hessinger 1988). *Erenna*
581 anisorhizas are also able to penetrate human skin and deliver a painful sting (Pugh 2001)
582 (and pers. obs.), a common feature of piscivorous cnidarians like cystonects or cubozoans.

583 (Thomason 1988) hypothesized that smaller, more spherical nematocysts, with a lower
584 surface area to volume ratio, are more efficient in osmotic-driven discharge and thus have

more power for skin penetration. The elongated haplonemes of crustacean-eating Tendiculophora have never been observed penetrating their crustacean prey ((Purcell 1984) and our unpublished observations), and are hypothesized to entangle the prey through adhesion of the abundant spines to the exoskeletal surfaces and appendages. Entangling requires less acceleration and power during discharge than penetration, as it does not rely on point pressure. In fish-eating cystonects and *Erenna* species, the haplonemes are much less elongated and very effective at penetration, in congruence with the osmotic discharge hypothesis. The accelerated rate of heteroneme shape diversification in the smallest clade containing *Agalma* and *Nanomia* may indicate a rapid dietary differentiation. However, our limited ecological data do not show any significant dietary differentiation in this group.

When we tested the diet-morphology correlation hypotheses supported in the literature from a macroevolutionary perspective, we found that most of them were consistent with correlated evolution (Table 2). The ecomorphological association between rhopalonemes, desmonemes, and crustacean eaters was not congruent with a scenario of correlated evolution. This could be due to the broader set of taxa in our analyses, including multiple species without desmonemes or rhopalonemes but which effectively capture crustaceans (such as *Cordagalma ordinatum*, *Lychnagalma utricularia*, and *Bargmannia amoena*).

While our results unambiguously show that tentillum morphology evolved with diet, the conclusions we can draw from these analyses are limited by the sparse dietary data available. Moreover, our analyses are not sufficient to adequately test hypotheses of adaptation, since that would require evidence of changes within a population exposed to different selective pressures. When interpreting these results, it is important to remember that diet is a product of environmental prey availability and predator selectivity. Selectivity differences across siphonophore species could be driven by other phenotypes not accounted for this study. For example, tentacle-deploying behavior, positioning in the water column, or thresholds for discharging on or ingesting an encountered animal. Further observations on these behaviors in the field are necessary to assess their relative importance in determining dietary composition.

612 In addition to behavior, there is much biochemistry in the prey capture and digestion processes
613 that remains unexplored. Part of the success in siphonophore prey capture is likely determined
614 by the effectiveness of the toxins delivered by the nematocysts on different taxa. Comparative
615 toxin assays and venom protein evolution studies could shed light on this question. Moreover,
616 siphonophore trophic specialization may have brought changes in the digestive biochemistry
617 of gastrozooids and palpons. A comparison of the gene expression levels for different enzymes
618 in the gastrozooids of different species, together with digestive enzyme sequence evolution
619 studies, and a toxicological assay of the different venoms in siphonophore nematocysts on
620 different prey taxa, would provide a great complement to our results.

621 *Generating hypotheses on siphonophore feeding ecology* – One motivation for our research
622 was to understand the links between predator capture tools and their diets so we can generate
623 hypotheses about the diets of siphonophores based on morphological characteristics. Indeed,
624 our discriminant analyses were able to distinguish between different siphonophore diets
625 based on morphological characters alone. The models produced by these analyses generated
626 testable predictions about the diets of many species for which we only have morphological
627 data of their tentacles. While the limited dataset used here is informative for generating
628 tentative hypotheses, the empirical data are still scarce and insufficient to cast robust
629 predictions. This reveals the need to extensively characterize siphonophore diets and feeding
630 habits. In future work, we can test these ecological hypotheses and validate these models
631 by directly characterizing the diets of some of those siphonophore species. Predicting diet
632 using morphology is a powerful tool to reconstruct food web topologies from community
633 composition alone. In many of the ecological models found in the literature, interactions
634 among the oceanic zooplankton have been treated as a black box (Mitra 2009). The ability
635 to predict such interactions, including those of siphonophores and their prey, will enhance
636 the taxonomic resolution of nutrient flow models constructed from plankton community
637 composition data.

638 *Phenotypic integration of siphonophore tentilla* – Tentillum characters, such as nema-

639 to cysts, arose from the subfunctionalization of serial homologs (David et al. 2008). Serial
640 homologs have shared genetic elements underlying their development, and are expected to
641 have phylogenetic correlations (Wagner and Schwenk 2000). In addition, these sub-structures
642 must fit and work together in synchrony to ensnare prey successfully (functional integration).
643 Character complexes that satisfy these conditions tend to be phenotypically integrated.
644 Phenotypic integration is the set of functional and genetic correlations among the traits of an
645 organism (Pigliucci 2003). These correlations have been hypothesized to direct and constrain
646 adaptive evolution (Wagner and Schwenk 2000). The siphonophore tentillum morphospace
647 has a fairly low extant dimensionality due to an evolutionary history with many synchronous,
648 correlated changes. This is consistent with strong phenotypic integration where genetic and
649 developmental correlations are maintained by natural selection to preserve function.

650 Part of the tentillum structural correlations are to be expected from shared regulatory
651 networks for elements that develop together from common positional bud (budding tentilla
652 in the tentacle). Similarly, correlations between nematocyst subtypes are also expected
653 given their common evolutionary and developmental origin. None of these explanations
654 for correlated evolution are surprising, nor require natural selection. However, we also
655 found correlations between nematocyst and tentillum characters. Siphonophore tentacle
656 nematocysts (in their cnidocytes) are not produced nor matured in the developing tentillum.
657 These cnidocytes are produced by dividing cnidoblasts in the basigaster (basal swelling
658 of the gastrozooid). Once the cnidocytes have assembled the nematocyst, they migrate
659 outward along the tentacle (Carré 1972) and position themselves in the tentillum according
660 to their type and size (Skaer 1988). Thus, the developmental programs that produce the
661 observed nematocyst morphologies are spatially separated from those producing the tentillum
662 morphologies. Therefore, we hypothesize the genetic correlations and phenotypic integration
663 between tentillum and nematocyst characters are maintained through natural selection on
664 separate regulatory networks, out of the necessity to work together and meet the spatial,
665 mechanical, and functional constraints of their prey capture behavior.

666 *Evolutionary history of tentillum morphology* – This study produced the most speciose
667 siphonophore molecular phylogeny to date, while incorporating the most recent findings in
668 siphonophore deep node relationships. This revealed for the first time that *Erenna* is the sister
669 to *Stephanomia amphytridis*. *Erenna* and *Stephanomia* bear the largest tentilla among all
670 siphonophores, thus their monophyly indicates that there was a single evolutionary transition
671 to giant tentilla. Siphonophore tentilla range in size from ~30 µm in some *Cordagalma*
672 specimens to 2-4 cm in *Erenna* species, and up to 8 cm in *Stephanomia amphytridis* (Pugh
673 and Baxter 2014). Most siphonophore tentilla measure between 175 and 1007 µm (1st and
674 3rd quartiles), with a median of 373 µm. The extreme gain of tentillum size in this newly
675 found clade may have important implications for access to large prey size classes.

676 Tentillum size, as well as the majority of the characters studied, supported BM evolutionary
677 models. There are two alternative hypotheses about the generative process of BM. One
678 hypothesis would suggest that these characters are not under selection, and therefore diverging
679 neutrally (Lande 1976). The second hypothesis suggests that they are under selection, but
680 the adaptive landscape was rapidly shifting (Hansen and Martins 1996), without leaving
681 clear patterns across the phylogeny. Some of the BM supported characters are likely to have
682 evolved under the second hypothesis, since when a diet-driven regime tree was provided,
683 these characters preferentially supported an OU model (Appendix 14).

684 Siphonophore tentilla are defined as lateral, monostichous evaginations of the tentacle
685 gastrovascular lumen with epidermal nematocysts (Totton and Bargmann 1965). The buttons
686 on *Physalia* tentacles were not traditionally regarded as tentilla, but (Bardi and Marques
687 2007) and our observations (Munro et al. 2018), confirm that the buttons contain evaginations
688 of the gastrovascular lumen, thus satisfying all the criteria for the definition. In this light,
689 and given that most Cystonectae bear conspicuous tentilla, we conclude (in agreement with
690 (Munro et al. 2018)) that tentilla are likely ancestral to all siphonophores, and secondarily
691 lost in *Apolemia* and *Bathyphysa conifera*.

692 The clade Tendiculophora contains far more species than its relatives Cystonectae, Apolemi-

693 idae, and Pyrostephidae. An increase in clade richness and ecological diversification can be
694 triggered by a ‘key innovation’ (Simpson 1955). The evolutionary innovation of the Tendicu-
695 lophora tentilla with shooting cnidobands and modular regions may have facilitated further
696 dietary diversification to unfold. In addition, our work identifies an interesting example of
697 convergent evolution. The calycophoran tentillum morphospace (Fig. 9) was independently
698 occupied by the physonect *Frillagalma vityazi*. Like calycophorans, *Frillagalma* tentilla have
699 small C-shaped cnidobands with a few rows of anisorhizas. Unlike calycophorans, they lack
700 paired elongate microbasic mastigophores. Instead, they bear three elongated stenoteles, and
701 their cnidobands are followed by a branched vesicle, unique to this genus. Their tentillum
702 morphology is very different from that of other related physonects, which tend to have long,
703 coiled, cnidobands with many paired oval stenoteles. Most calycophoran diet studies have
704 reported their prey to be small crustaceans such as copepods or ostracods. The diet of
705 *Frillagalma vityazi* is unknown, but this morphological convergence presents the hypothesis
706 that they evolved to capture similar kinds of prey. Our DAPCs predict that *Frillagalma* has
707 a generalist niche with both soft and hard bodied prey, including copepods.

708 *Evolution of nematocyst shape* – The phylogenetic placement of siphonophores among
709 the Hydrozoa remains an unresolved question (Munro et al. 2018). The most recent
710 work on this front sets them as sister group to all other Hydroidolina (Kayal et al. 2015).
711 All reconstructions of hydrozoan relationships recover siphonophores as an early diverging
712 lineage within Hydroidolina, with many unique apomorphic characters. Therefore, there
713 is a great uncertainty around the ancestral plesiomorphies of the common ancestor of all
714 siphonophores. This is especially true for those characters that present extreme differences
715 between Cystonectae and Codonophora (the earliest split in the siphonophore phylogeny). One
716 such character is the shape of haploneme nematocysts. A remarkable feature of siphonophore
717 haplonemes is that they are outliers to all other Medusozoa in their surface area to volume
718 relationships, deviating significantly from sphericity (Thomason 1988). This suggests a
719 different mechanism for their discharge that could be more reliant on capsule tension than

720 on osmotic potentials (Carré and Carré 1980), and strong selection for efficient nematocyst
721 packing in the cnidoband (Thomason 1988; Skaer 1988). Our results show that Codonophora
722 underwent a shift towards elongation and Cystonectae towards sphericity, assuming the
723 common ancestor had an intermediate state. Since we know that the haplonemes of other
724 hydrozoan outgroups are generally spheroid, it is more parsimonious to assume that cystonects
725 retain this ancestral state. Later, we observe a return to more rounded (ancestral) haplonemes
726 in *Erenna*, associated with a secondary gain of a piscivorous trophic niche, like that exhibited
727 by cystonects.

728 Simultaneous with this shift in haploneme shape, heteroneme shape evolution also presents
729 a single transition to elongation. In addition, the clade defined by the most recent common
730 ancestor of *Agalma* and *Nanomia* shows an increased rate of divergence for heteroneme shape,
731 spanning extremes (from oval *Nanomia* stenoteles to the elongate *Agalma okenii* stenoteles)
732 in relatively short evolutionary time. While cystonects do not bear heteronemes in their
733 tentacles, *Physalia physalis* bears stenoteles in other zooids, hypothetically used for defense
734 rather than for prey capture. These stenotele heteronemes are rounded like those found in
735 pyrostephids and apolemiids, which is consistent with the story of a single transition leading
736 to the elongated heteronemes in the stem of Tendiculophora.

737 The implications of these results to the evolution of nematocyst function suggests that an
738 innovation in the discharge mechanism of haplonemes may have occurred during the main shift
739 to elongation. Elongate nematocysts can be tightly packed into cnidobands. We hypothesize
740 this may be a Tendiculophora lineage-specific adaptation to packing more nematocysts into a
741 limited tentillum space, as suggested by (Skaer 1988). Tendiculophora is the most abundant,
742 speciose, and diverse (ecologically and morphologically) clade of siphonophores, containing
743 the clades Euphysonectae and Calycophorae. We hypothesize that this packing-efficient
744 haploeme morphology may have been a key innovation leading to the diversification of this
745 clade. However, other characters that shifted concurrently in the stem of this clade may have
746 been responsible for their extant diversity.

747 Some siphonophore clades have more nematocyst types than others in the tentacles
748 (Tendiculophora has 4 types, Cystonectae and Apolemiidae have 1), or different subtypes
749 (e.g. stenoteles, mastigophores, birhopaloids). Siphonophores bear nematocysts in different
750 parts of the colony (tentacles, gastrozooids, papons, palpacles, bracts, nectophores, and
751 gonozoooids) (Totton and Bargmann 1965). In this paper we only look at the presence of
752 nematocyst types in the tentacles, therefore the gains and losses reported are not necessarily
753 morphological innovations, but developmental allocations. For instance, stenoteles (a type of
754 heteroneme) are absent from the tentacles of *Physalia* and seem to reappear in Euphysonectae,
755 but we know that *Physalia* has stenoteles in other body parts (Totton and Bargmann 1965).
756 Nonetheless, siphonophores have evolved unique nematocyst types and subtypes, not present
757 in any other cnidarian, such as the two types of rhopalonemes (acrophores and anacrophores),
758 and the haploneme homotrichous anisorrhizas (Werner 1965). Both these nematocyst types
759 evolved in the stem to Tendiculophora, and are likely morphological innovations, since they
760 have not been yet found in any other tissue of any other organism. The gain of extreme
761 elongation in the haplonemes of Tendiculophora can be interpreted as part of the character
762 shift to a novel anisorrhiza subtype.

763 *Diversity of discharge dynamics* – A fundamental corollary in functional morphology is
764 that structural morphology determines functional performance (Wainwright and Reilly 1994).
765 We expected the discharge dynamics exhibited by siphonophore tentilla should vary with their
766 morphological diversity. Our results are consistent with this expectation, and we observe,
767 for example, that cnidoband size largely correlates with cnidoband discharge speed. This
768 suggests that prey escape response speed may determine the minimum cnidoband length for
769 successful capture.

770 *Insights from tentillum morphology* – The measurements taken illustrate that the morpho-
771 logical diversity of siphonophore tentilla and nematocysts spans clades, from the overall shape
772 and size, to the dimensions of the nematocysts. Siphonophores bear the largest nematocysts
773 among Hydrozoans, and present a wide variety of nematocyst sizes within the clade. The

⁷⁷⁴ largest nematocysts in our dataset (*Bargmannia lata* by volume and *Resomia dunni* by
⁷⁷⁵ length), are the largest of all nematocysts reported for cnidarians, and therefore possibly the
⁷⁷⁶ largest intracellular organelles among all living things.

⁷⁷⁷ In addition to the insights produced in this study, the newly collected morphological
⁷⁷⁸ data provide a unique resource for future studies, and a reference dataset for siphonophore
⁷⁷⁹ identification. Many conspicuous categorical characters in siphonophore tentilla are very
⁷⁸⁰ diagnostic, such as: the fluorescent lures of *Resomia ornicephala*, the bioluminescent lures
⁷⁸¹ of *Erenna* species, the unique branched vesicle of *Frillagalma vityazi*, the buoyant medusa-
⁷⁸² resembling vesicle of *Lychnagalma* with 8 pseudo-tentacles, the zig-zag morphology of *Resomia*
⁷⁸³ species, the inverted orientation of *Physophora* cnidobands, the button-like tentilla of *Physalia*,
⁷⁸⁴ or the acorn-shaped minute tentilla of *Cordagalma* species (Fig. 7). Some categorical
⁷⁸⁵ characters are synapomorphic diagnostic characters for large clades, such as the proximal
⁷⁸⁶ tentillum heteronemes of Eucladophora, the elastic strand, rhopalonemes, and desmonemes of
⁷⁸⁷ Tendiculophora, the larval tentilla of Euphysonectae, the two-sized isorhizas of Cystonectae,
⁷⁸⁸ the saccus canal of Pyrostephidae, or the seven rows of anisorhizas in Calycophorae. These
⁷⁸⁹ characters should be used together with the classical nectophore and bract characters to
⁷⁹⁰ identify species or at least impute phylogenetic affiliation from incomplete material.

⁷⁹¹ **Conclusions**

⁷⁹² Siphonophores have diverse predatory niches in the open ocean, ranging from mid-trophic
⁷⁹³ small crustacean eaters to piscivorous super-carnivores. With the evolution of diversified
⁷⁹⁴ prey type specializations comes the evolution of morphologies adapted to the challenges
⁷⁹⁵ posed by different prey. The results presented here indicate that the associations found
⁷⁹⁶ between siphonophore tentilla and their prey are a product of correlated evolution in highly
⁷⁹⁷ integrated traits. While much of the literature focuses on how predatory generalists evolve
⁷⁹⁸ into predatory specialists, in siphonophores we find predatory specialists can evolve into
⁷⁹⁹ generalists, and that specialists on one prey type have directly evolved into specialists on

800 other prey types. Our extended morphological characterization shows that the relationships
801 between form and ecology hold across a large set of taxa and characters, and can be used to
802 generate hypotheses on the feeding habits of uncharacterized species. We conclude that the
803 siphonophores were able to establish as abundant oceanic predators by occupying a variety of
804 trophic niches facilitated by the evolution and diversification of extraordinary prey capture
805 tools on their tentacles.

806 **Supplementary Materials**

807 Data available from the Dryad Digital Repository: <http://dx.doi.org/10.5061/dryad.NNNN>
808 Online Appendices are available in https://github.com/dunnlab/tentilla_morph/
809 Supplementary_materials/Online_Appendices

810 **Funding**

811 This work was supported by the Society of Systematic Biologists (Graduate Student Award
812 to A.D.S.); the Yale Institute of Biospheric Studies (Doctoral Pilot Grant to A.D.S.); and
813 the National Science Foundation (Waterman Award to C.W.D., and NSF-OCE 1829835 to
814 C.W.D., S.H.D.H., and C. Anela Choy). A.D.S. was supported by a Fulbright Spain Graduate
815 Studies Scholarship.

816 **Acknowledgements**

817 We wish to thank the crew and scientists of the R/V Western Flyer, who participated in
818 the collection of many of the specimens used in this study. We also want to thank Lynne
819 Christianson and Shannon Johnson from the Monterey Bay Aquarium Research Institute
820 for their assistance in the field as well as for sequencing some of the species included in this
821 phylogeny. In addition, we wish to thank Lourdes Rojas, Daniel Drew, and Eric Lazo-Wasem
822 for their assistance in imaging the fixed specimens and managing the collections. We thank

823 Dennis Pilarczyk for organizing the prey selectivity data, and Joaquin Nunez for reviewing
824 this manuscript. Furthermore, we thank Elizabeth D. Hetherington and C. Anela Choy
825 for collating the data on siphonophore feeding and for reviewing the manuscript. Finally,
826 we thank Philip Pugh, who confirmed many of our specimen identifications and taught us
827 valuable knowledge about siphonophores.

828 References

- 829 Adams D.C., Collyer M., Kaliontzopoulou A., Sherratt E. 2016. Geomorph: Software for
830 geometric morphometric analyses..
- 831 Andersen O.G.N. 1981. Redescription of marrus orthocanna (kramp, 1942)(Cnidaria,
832 siphonophora). Zoological Museum, University of Copenhagen.
- 833 Bardi J., Marques A.C. 2007. Taxonomic redescription of the portuguese man-of-war,
834 physalia physalis (cnidaria, hydrozoa, siphonophorae, cystonectae) from brazil. Iheringia.
835 Série Zoologia. 97:425–433.
- 836 Beaulieu J., O'Meara B. 2012. OUwie: Analysis of evolutionary rates in an ou framework.
837 R package version 1.17..
- 838 Biggs D.C. 1977. Field studies of fishing, feeding, and digestion in siphonophores. Marine
839 & Freshwater Behaviour & Phy. 4:261–274.
- 840 Blomberg S.P., Garland T., Ives A.R. 2003. Testing for phylogenetic signal in comparative
841 data: Behavioral traits are more labile. Evolution. 57:717–745.
- 842 Blyth C.R. 1972. On simpson's paradox and the sure-thing principle. Journal of the
843 American Statistical Association. 67:364–366.
- 844 Butler M.A., King A.A. 2004. Phylogenetic comparative analysis: A modeling approach
845 for adaptive evolution. The American Naturalist. 164:683–695.
- 846 Carré D. 1972. Study on development of cnidocysts in gastrozooids of muggiaeae kochi
847 (will, 1844) (siphonophora, calycophora). Comptes Rendus Hebdomadaires des Seances de
848 l'Academie des Sciences Serie D. 275:1263.

- 849 Carré D., Carré C. 1980. On triggering and control of cnidocyst discharge. *Marine &*
850 *Freshwater Behaviour & Phy.* 7:109–117.
- 851 Choy C.A., Haddock S.H., Robison B.H. 2017. Deep pelagic food web structure as revealed
852 by in situ feeding observations. *Proceedings of the Royal Society B: Biological Sciences.*
853 284:20172116.
- 854 Collins T.J. 2007. ImageJ for microscopy. *Biotechniques.* 43:S25–S30.
- 855 Costello J.H., Colin S.P., Gemmell B.J., Dabiri J.O., Sutherland K.R. 2015. Multi-jet
856 propulsion organized by clonal development in a colonial siphonophore. *Nature communica-*
857 *tions.* 6:8158.
- 858 Cressler C.E., Butler M.A., King A.A. 2015. Detecting adaptive evolution in phylogenetic
859 comparative analysis using the ornstein–uhlenbeck model. *Systematic biology.* 64:953–968.
- 860 David C.N., Özbek S., Adamczyk P., Meier S., Pauly B., Chapman J., Hwang J.S.,
861 Gojobori T., Holstein T.W. 2008. Evolution of complex structures: Minicollagens shape the
862 cnidarian nematocyst. *Trends in genetics.* 24:431–438.
- 863 Dunn C.W., Pugh P.R., Haddock S.H. 2005. Molecular phylogenetics of the siphonophora
864 (cnidaria), with implications for the evolution of functional specialization. *Systematic biology.*
865 54:916–935.
- 866 Felsenstein J. 1985. Phylogenies and the comparative method. *The American Naturalist.*
867 125:1–15.
- 868 Futuyma D.J., Moreno G. 1988. The evolution of ecological specialization. *Annual review*
869 *of Ecology and Systematics.* 19:207–233.
- 870 Grafen A. 1989. The phylogenetic regression. *Philosophical Transactions of the Royal*
871 *Society of London. B, Biological Sciences.* 326:119–157.
- 872 Haddock S.H., Dunn C.W. 2015. Fluorescent proteins function as a prey attractant:
873 Experimental evidence from the hydromedusa olindias formosus and other marine organisms.
874 *Biology open.* 4:1094–1104.
- 875 Haddock S.H., Dunn C.W., Pugh P.R., Schnitzler C.E. 2005. Bioluminescent and red-

- 876 fluorescent lures in a deep-sea siphonophore. *Science*. 309:263–263.
- 877 Haddock S.H., Heine J.N. 2005. Scientific blue-water diving. California Sea Grant College
878 Program.
- 879 Hansen T.F., Martins E.P. 1996. Translating between microevolutionary process and
880 macroevolutionary patterns: The correlation structure of interspecific data. *Evolution*.
881 50:1404–1417.
- 882 Hardin G. 1960. The competitive exclusion principle. *science*. 131:1292–1297.
- 883 Harmon L.J., Losos J.B., Jonathan Davies T., Gillespie R.G., Gittleman J.L., Bryan
884 Jennings W., Kozak K.H., McPeek M.A., Moreno-Roark F., Near T.J., others. 2010. Early
885 bursts of body size and shape evolution are rare in comparative data. *Evolution: International*
886 *Journal of Organic Evolution*. 64:2385–2396.
- 887 Harmon L.J., Weir J.T., Brock C.D., Glor R.E., Challenger W. 2007. GEIGER: Investi-
888 gating evolutionary radiations. *Bioinformatics*. 24:129–131.
- 889 Hessinger D.A. 1988. Nematocyst venoms and toxins. *The biology of nematocysts*.
890 Elsevier. p. 333–368.
- 891 Hissmann K. 2005. In situ observations on benthic siphonophores (physonectae: Rhodali-
892 idae) and descriptions of three new species from indonesia and south africa. *Systematics and*
893 *Biodiversity*. 2:223–249.
- 894 Hoberg E.P., Brooks D.R. 2008. A macroevolutionary mosaic: Episodic host-switching,
895 geographical colonization and diversification in complex host–parasite systems. *Journal of*
896 *Biogeography*. 35:1533–1550.
- 897 Höhna S., Landis M.J., Heath T.A., Boussau B., Lartillot N., Moore B.R., Huelsenbeck
898 J.P., Ronquist F. 2016. RevBayes: Bayesian phylogenetic inference using graphical models
899 and an interactive model-specification language. *Systematic Biology*. 65:726–736.
- 900 Hutchinson G.E. 1961. The paradox of the plankton. *The American Naturalist*. 95:137–
901 145.
- 902 Jacobs J. 1974. Quantitative measurement of food selection. *Oecologia*. 14:413–417.

- 903 Johnson K.P., Malenke J.R., Clayton D.H. 2009. Competition promotes the evolution of
904 host generalists in obligate parasites. *Proceedings of the Royal Society B: Biological Sciences.*
905 276:3921–3926.
- 906 Jombart T., Devillard S., Balloux F. 2010. Discriminant analysis of principal components:
907 A new method for the analysis of genetically structured populations. *BMC genetics.* 11:94.
- 908 Kalyaanamoorthy S., Minh B.Q., Wong T.K., Haeseler A. von, Jermiin L.S. 2017. Mod-
909 elFinder: Fast model selection for accurate phylogenetic estimates. *Nature methods.* 14:587.
- 910 Katoh K., Misawa K., Kuma K.-i., Miyata T. 2002. MAFFT: A novel method for
911 rapid multiple sequence alignment based on fast fourier transform. *Nucleic acids research.*
912 30:3059–3066.
- 913 Kayal E., Bentlage B., Cartwright P., Yanagihara A.A., Lindsay D.J., Hopcroft R.R.,
914 Collins A.G. 2015. Phylogenetic analysis of higher-level relationships within hydroidolina
915 (cnidaria: Hydrozoa) using mitochondrial genome data and insight into their mitochondrial
916 transcription. *PeerJ.* 3:e1403.
- 917 Lande R. 1976. Natural selection and random genetic drift in phenotypic evolution.
918 *Evolution.* 30:314–334.
- 919 Longhurst A.R. 1985. The structure and evolution of plankton communities. *Progress in*
920 *Oceanography.* 15:1–35.
- 921 Mackie G.O., Pugh P.R., Purcell J.E. 1987. Siphonophore Biology. *Advances in Marine*
922 *Biology.* 24:97–262.
- 923 Mapstone G.M. 2014. Global diversity and review of siphonophorae (cnidaria: Hydrozoa).
924 *PLoS One.* 9:e87737.
- 925 Martins E.P. 1996. Phylogenies, spatial autoregression, and the comparative method: A
926 computer simulation test. *Evolution.* 50:1750–1765.
- 927 Mitra A. 2009. Are closure terms appropriate or necessary descriptors of zooplankton loss
928 in nutrient–phytoplankton–zooplankton type models? *Ecological Modelling.* 220:611–620.
- 929 Munro C., Siebert S., Zapata F., Howison M., Serrano A.D., Church S.H., Goetz F.E.,

- 930 Pugh P.R., Haddock S.H., Dunn C.W. 2018. Improved phylogenetic resolution within
931 siphonophora (cnidaria) with implications for trait evolution. Molecular Phylogenetics and
932 Evolution.
- 933 Nguyen L.-T., Schmidt H.A., Haeseler A. von, Minh B.Q. 2014. IQ-tree: A fast and
934 effective stochastic algorithm for estimating maximum-likelihood phylogenies. Molecular
935 biology and evolution. 32:268–274.
- 936 O'Brien T.D. 2007. COPEPOD, a global plankton database: A review of the 2007
937 database contents and new quality control methodology..
- 938 Pagel M. 1994. Detecting correlated evolution on phylogenies: A general method for the
939 comparative analysis of discrete characters. Proceedings of the Royal Society of London.
940 Series B: Biological Sciences. 255:37–45.
- 941 Paradis E., Blomberg S., Bolker B., Brown J., Claude J., Cuong H.S., Desper R. 2019.
942 Package “ape”. Analyses of phylogenetics and evolution, version.:2–4.
- 943 Pennell M.W., FitzJohn R.G., Cornwell W.K., Harmon L.J. 2015. Model adequacy and
944 the macroevolution of angiosperm functional traits. The American Naturalist. 186:E33–E50.
- 945 Pigliucci M. 2003. Phenotypic integration: Studying the ecology and evolution of complex
946 phenotypes. Ecology Letters. 6:265–272.
- 947 Pugh P. 2001. A review of the genus erenna bedot, 1904 (siphonophora, physonectae).
948 BULLETIN-NATURAL HISTORY MUSEUM ZOOLOGY SERIES. 67:169–182.
- 949 Pugh P., Baxter E. 2014. A review of the physonect siphonophore genera halistemma
950 (family agalmatidae) and stephanomia (family stephanomiidae). Zootaxa. 3897:1–111.
- 951 Pugh P., Youngbluth M. 1988. Two new species of prayine siphonophore (calycophorae,
952 prayidae) collected by the submersibles johnson-sea-link i and ii. Journal of Plankton Research.
953 10:637–657.
- 954 Purcell J. 1981. Dietary composition and diel feeding patterns of epipelagic siphonophores.
955 Marine Biology. 65:83–90.
- 956 Purcell J.E. 1980. Influence of siphonophore behavior upon their natural diets: Evidence

- 957 for aggressive mimicry. *Science*. 209:1045–1047.
- 958 Purcell J.E. 1984. The functions of nematocysts in prey capture by epipelagic
959 siphonophores (coelenterata, hydrozoa). *The Biological Bulletin*. 166:310–327.
- 960 Purcell J., Mills C. 1988. The correlation of nematocyst types to diets in pelagic hydrozoa.
961 In “the biology of nematocysts”.(Eds da hessinger and hm lenhoff.) pp. 463–485..
- 962 Rabosky D.L., Grunbler M., Anderson C., Title P., Shi J.J., Brown J.W., Huang H.,
963 Larson J.G. 2014. BAMM tools: An r package for the analysis of evolutionary dynamics on
964 phylogenetic trees. *Methods in Ecology and Evolution*. 5:701–707.
- 965 Revell L.J. 2012. Phytools: An r package for phylogenetic comparative biology (and other
966 things). *Methods in Ecology and Evolution*. 3:217–223.
- 967 Revell L.J., Chamberlain S.A. 2014. Rphylip: An r interface for phylip. *Methods in
968 Ecology and Evolution*. 5:976–981.
- 969 Revell L.J., Collar D.C. 2009. Phylogenetic analysis of the evolutionary correlation using
970 likelihood. *Evolution: International Journal of Organic Evolution*. 63:1090–1100.
- 971 Robison B.H. 2004. Deep pelagic biology. *Journal of experimental marine biology and
972 ecology*. 300:253–272.
- 973 Schindelin J., Arganda-Carreras I., Frise E., Kaynig V., Longair M., Pietzsch T., Preibisch
974 S., Rueden C., Saalfeld S., Schmid B., others. 2012. Fiji: An open-source platform for
975 biological-image analysis. *Nature methods*. 9:676.
- 976 Schluter D. 2000. Ecological character displacement in adaptive radiation. *the american
977 naturalist*. 156:S4–S16.
- 978 Schmitz O. 2017. Predator and prey functional traits: Understanding the adaptive
979 machinery driving predator–prey interactions. *F1000Research*. 6.
- 980 Shapiro S.S., Wilk M.B. 1965. An analysis of variance test for normality (complete
981 samples). *Biometrika*. 52:591–611.
- 982 Siebert S., Pugh P.R., Haddock S.H., Dunn C.W. 2013. Re-evaluation of characters in
983 apolemiidae (siphonophora), with description of two new species from monterey bay, california.

- 984 Zootaxa. 3702:201–232.
- 985 Simpson G.G. 1944. Tempo and mode in evolution. Columbia University Press.
- 986 Simpson G.G. 1955. Major features of evolution. Columbia University Press: New York.
- 987 Skaer R. 1988. The formation of cnidocyte patterns in siphonophores. Academic Press
- 988 New York.
- 989 Skaer R. 1991. Remodelling during the development of nematocysts in a siphonophore.
- 990 Hydrobiologia. 216:685–689.
- 991 Stireman-III J.O. 2005. The evolution of generalization? Parasitoid flies and the perils of
- 992 inferring host range evolution from phylogenies. Journal of evolutionary biology. 18:325–336.
- 993 Sugiura N. 1978. Further analysts of the data by akaike's information criterion and the
- 994 finite corrections: Further analysts of the data by akaike's. Communications in Statistics-
- 995 Theory and Methods. 7:13–26.
- 996 Team R.C. 2017. R: A language and environment for statistical computing. Vienna,
- 997 austria: R foundation for statistical computing; 2017..
- 998 Thomason J. 1988. The allometry of nematocysts. The biology of nematocysts. Elsevier.
- 999 p. 575–588.
- 1000 Totton A.K., Bargmann H.E. 1965. A synopsis of the siphonophora. British Museum
- 1001 (Natural History).
- 1002 Uhlenbeck G.E., Ornstein L.S. 1930. On the theory of the brownian motion. Physical
- 1003 review. 36:823.
- 1004 Uyeda J.C., Zenil-Ferguson R., Pennell M.W. 2018. Rethinking phylogenetic comparative
- 1005 methods. Systematic Biology. 67:1091–1109.
- 1006 Wagner G.P., Schwenk K. 2000. Evolutionarily stable configurations: Functional in-
- 1007 tegration and the evolution of phenotypic stability. Evolutionary biology. Springer. p.
- 1008 155–217.
- 1009 Wainwright P.C., Reilly S.M. 1994. Ecological morphology: Integrative organismal biology.
- 1010 University of Chicago Press.

₁₀₁₁ Werner B. 1965. Die nesselkapseln der cnidaria, mit besonderer berücksichtigung der
₁₀₁₂ hydroida. Helgoländer wissenschaftliche Meeresuntersuchungen. 12:1.